Large Quadratic Hyperpolarizabilities with Donor–Acceptor Polyenes Exhibiting Optimum Bond Length Alternation: Correlation between Structure and Hyperpolarizability

M. Blanchard-Desce,* V. Alain, P. V. Bedworth, S. R. Marder, A. Fort, C. Runser, M. Barzoukas, S. Lebus, and R. Wortmann

Abstract: Donor–acceptor polyenes of various lengths, and that combine aromatic electron-donating moieties with powerful heterocyclic electron-withdrawing terminal groups, have been synthesized and characterized as efficient nonlinear optical (NLO) chromophores. Their linear and nonlinear optical properties have been investigated, and variations in these properties have been related to ground-state polarization (dipole μ) and structure. In particular, unprecedented quadratic hyperpolarizabilities (β) have been achieved (up to $\beta(0) = 1500 \times 10^{-30}$ esu) by reduction of the bond-length alternation (BLA) in the polyenic chain. In each series of homologous compounds, increasing the number n of conjugated double bonds in the polyenic chain results in a marked bathochromic shift, more pronounced BLA, and exponential increases in $\mu\beta(0)$ values. As a result, polyenic chromophores displaying excellent optical quadratic nonlinearities (with $\mu\beta$ values as large as 100 times that of the quadratic NLO benchmark 4-dimethyl-amino-4'-nitrostilbene (DANS)), as well as satisfactory solubility, have been obtained.

Keywords

chromophores · donor–acceptor systems · hyperpolarizability · nonlinear optics · polyenes

Introduction

The elaboration of nonlinear optical (NLO) materials has attracted considerable interest for the past two decades because of their potential applications in telecommunications, optical data storage, and optical information processing. In particular, organic materials have received much attention.[1–8] Organic crystals now exist with higher nonlinearities than inorganic crystals such as lithium niobate ($LiNbO_3$). Organic materials also provide an excellent basis for the optimization of NLO materials owing to their combination of chemical flexibility with a variety of possible processing strategies.

Second-order NLO effects such as second harmonic generation (SHG) or electrooptic modulation (which allows for modulation of the refractive indices of materials by application of an electric static field) require the design of NLO chromophores that exhibit large molecular quadratic hyperpolarizability (β). In particular, there is currently a need for highly nonlinear organic chromophores with large ground-state dipole moments as active elements in poled-polymer-based systems for electrooptic modulation.

Most attempts to design molecules with large β have been based upon "push–pull" compounds. Such chromophores have an electron-donating group and an electron-withdrawing group that interact through a π-conjugated system (with p-nitroaniline as the prototype molecular structure). These molecules can display a large quadratic hyperpolarizability owing to the occurrence of an intramolecular charge transfer (ICT) transition. Within the two-level approximation, the quadratic hyperpolarizability tensor β_{ijk} is fully one-dimensional along the donor–acceptor ICT axis, its main component β being related to ICT transition characteristics according to Equation (1).[9, 10] For

$$\beta(0) = \frac{3\mu_{01}^2 \Delta\mu}{2E_{01}^2} \tag{1}$$

push–pull molecules, the quadratic hyperpolarizability β is thus expected to increase with decreasing ICT transition energy (E_{01}), increasing transition dipole (μ_{01}) and increasing change of dipole moment upon excitation ($\Delta\mu$ being the difference between excited-state and ground-state dipole moments). However, molecular engineering of push–pull systems for quadratic

[*] Dr. M. Blanchard-Desce, V. Alain
Département de Chimie, Ecole Normale Supérieure (URA 1679 CNRS)
24 rue Lhomond, F-75231 Paris Cedex 05 (France)
Fax: Int. code +(1)44323325
e-mail: mbdesce@chimene.ens.fr
Dr. P. V. Bedworth, Dr. S. R. Marder
The Beckman Institute, California Institute of Technology
Pasadena, CA 91125 (USA)
Dr. A. Fort, Dr. C. Runser, Prof. M. Barzoukas
Institut de Physique et Chimie des Matériaux de Strasbourg
Groupe d'Optique Nonlinéaire et d'Optoélectronique (UMR 046 CNRS)
23 rue du Loess, F-67037 Strasbourg Cedex (France)
Dr. S. Lebus, Dr. R. Wortmann
Institut für Physikalische Chemie der Universität Mainz
Jakob Welder-Weg 11, D-55099 Mainz (Germany)

NLO is not straightforward since these parameters are interrelated. Therefore, we have attempted to rationally design optimized push–pull systems by tuning the end groups, as well as the length and structure of the conjugated system.

Results and Discussion

Design: First, we chose to focus on push–pull polyenes, since several recent experimental studies have emphasized the superiority of the polyenic system in terms of quadratic nonlinearities and showed that increasing the polyenic chain length results in pronounced increases in the quadratic hyperpolarizability.[11–23] This effect can be related to the red shift of the ICT transition as well as to the concomitant increases of both the transition dipole and the photoinduced change in dipole ($\Delta\mu$) that have been demonstrated experimentally for several series of push–pull phenylpolyenes and diphenylpolyenes of increasing size.[24, 25] Previous experimental studies also demonstrated that the nature of the end groups strongly influences both the magnitude of β and its chain-length behavior.[11, 15, 18, 21–24] Thus, appropriate choice of donor and acceptor terminal groups is expected to further enhance the quadratic hyperpolarizability of push–pull polyenes.

In addition, semiempirical calculations performed on push–pull polyenes have shown that the static quadratic hyperpolarizability can be correlated with the ground-state polarization and concomitantly with a structural parameter, the bond length alternation (BLA).[26–28] This coordinate describes the ground-state geometry of the molecule and is defined as the average difference in length between adjacent carbon–carbon bonds in the polyenic chain. The calculations indicate that the quadratic hyperpolarizability drops for highly alternated structures (BLA = ±0.11 Å, corresponding to alternating long (1.45 Å) single and short (1.34 Å) double bonds) and cancels when BLA = 0 Å (i.e., for nonalternated structures). On the other hand, β peaks at *intermediate* BLA values (BLA = $\pm0.05\pm0.01$ Å), the corresponding magnitude $|\beta_{max}|$ of the positive and negative extrema being system-dependent (see Figure 1). Consequently, for a given polyenic chain length, a suit-

Abstract in French: *Dans le cadre de l'élaboration de chromophores pour l'optique nonlinéaire, des polyènes "push–pull" présentant des groupements électrodonneurs aromatiques et des groupes électroattracteurs hétérocycliques ont été préparés et étudiés. Leurs propriétés optiques peuvent être corrélées à la structure (en particulier l'alternance de longueur de liaison au sein de la chaîne conjuguée) et la polarisation de l'état fondamental. Pour chaque série de composés homologues, l'allongement de la chaîne polyénique s'accompagne d'un effet bathochrome et d'une augmentation exponentielle de la réponse nonlinéaire. L'optimisation de la structure "push–pull" a été effectuée en jouant sur l'alternance de longueur de liaison et l'effet de taille. Cette approche a permis d'accéder à des chromophores solubles présentant des non-linéarités quadratiques exceptionnelles ($\beta(0)$ = 1500×10^{-30} esu et des valeurs de $\mu\beta$ atteignant 100 fois celle du 4-diméthylamino-4'-nitrostilbène (DANS)).*
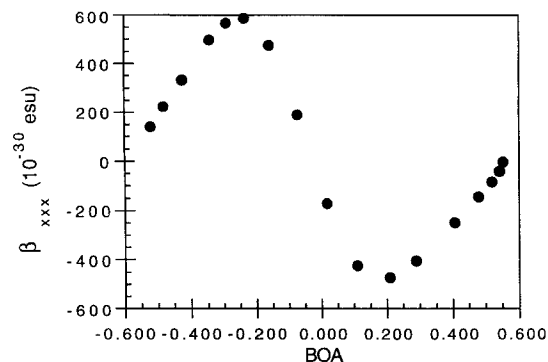
Figure 1. Dependence of β on the ground-state geometry for $(Me)_2N-(CH=CH)_4-CHO$. BOA is the bond order alternation as defined in refs. [27,28].

able combination of donor–acceptor groups ensuring optimum $|BLA|$, as well as simultaneously large $|\beta_{max}|$ value, is required to achieve markedly enhanced quadratic hyperpolarizability. It should be added that $|\beta_{max}|$ value depends on the structure and length of the π-conjugated system, as well as on the nature of the donor and acceptor groups.[26, 29]

In a simplified description of push–pull polyenes as mixtures of neutral and charge-separated (zwitterionic) limiting resonance forms (Figure 2), it can easily be realized that both the
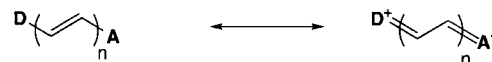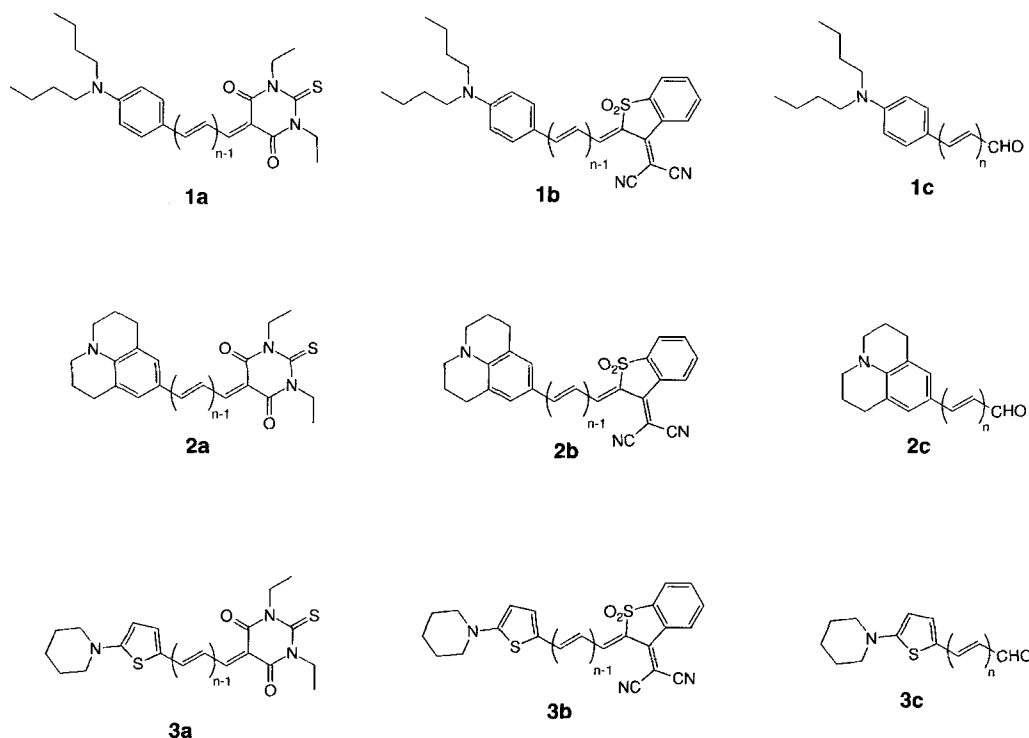

Figure 2. Neutral (left) and zwitterionic (right) limiting resonance forms of push–pull polyenes.

geometrical structure (i.e., BLA) and the polarization (i.e., ground-state dipole) are interrelated. Both of them are determined by the mixing between the two limiting resonance forms. If the neutral form prevails in the ground-state structure, BLA is defined as negative. Its value can range from -0.11 Å to 0 Å. Conversely, if the zwitterionic form prevails in the ground state, the sign of the coordinate is positive and can vary from 0 Å up to $+0.11$ Å. When both forms contribute equally to the molecular structure, there is no bond length alternation (i.e. BLA = 0 Å). This particular case is referred to as the "cyanine limit", by analogy with symmetrical cyanines that can be described as equal mixtures of two degenerate limiting resonance forms.
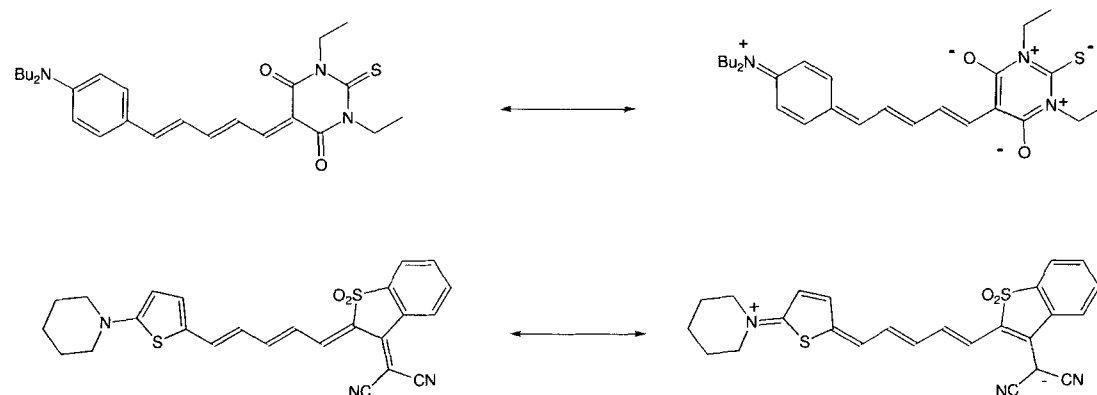
Thus, by tuning the parameters that govern the relative weight of the two limiting resonance forms, it should be possible to optimize the molecular structure so as to maximize the optical nonlinearities.[30] Qualitatively, a number of factors such as the donor–acceptor strength, the nature and size of the conjugated path, and external perturbations dictate the balance between the limiting resonance forms. For instance, for a given molecular structure, increasing the donor–acceptor strength will tend to increase charge separation. In contrast, increasing length will tend to disfavor charge separation. Aromaticity is also an important factor that will favor the limiting resonance form with the larger aromatic stabilization. Likewise, in solution increasing solvent polarity can stabilize charge separation. Thus, guidelines are available for the tuning of the nonlinear molecular

Scheme 1. Structural formulae of the series of push–pull polyenes investigated.

aimed at reaching the optimum mixing required to yield enhanced quadratic optical responses. In addition, donors of different strength were selected so as to tune the basic structure about optimum |BLA| value. For instance, the loss in aromatic stabilization in the donor end upon charge separation should be smaller for the thiophene ring (series 3) than for a phenyl ring (series 1 and 2), so that a more pronounced contribution from the zwitterionic form is expected for derivatives 3 than for derivatives 1 and 2. Also, the julolidine donor moiety ring (series 2) is known to behave as a stronger donor than the classical dimethylanilino moiety.

responses by modulating the mixing between the two limiting resonance forms, and therefore for the engineering of molecular structures with optimum BLA and enhanced quadratic optical nonlinearities.

Within this framework, we have designed several series of push–pull polyenes that incorporate aromatic electron-donating moieties and heterocyclic electron-withdrawing end groups (series 1–3a, 1–3b in Scheme 1). In order to make up for the loss in aromaticity on the donor side upon charge separation, we chose powerful heterocyclic acceptors[19, 31–33] such as the 1,3-diethyl-2-thiobarbituric acid moiety, which gains aromatic stabilization upon charge separation (see Figure 3). We also examined the 3-(dicyanomethylidenyl)-2,3-dihydrobenzothiophene-2-ylidenyl-1,1-dioxide acceptor moiety, whose phenyl ring becomes conjugated with the polyenic chain in the charge-separated form (see Figure 3). By combining aromatic donor groups with acceptors that bring some stabilization in the zwitterionic form, we sought to achieve reduced bond length alternation and
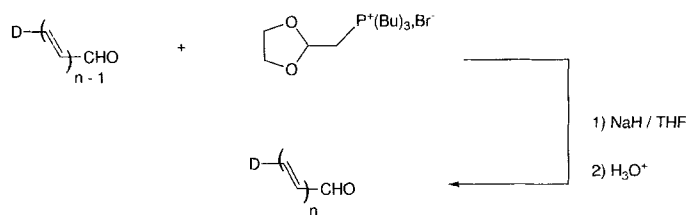
Moreover, we have investigated series of analogous derivatives of increasing length, so as to achieve even larger hyperpolarizabilities. Examination of these series helps to increase our understanding of the factors that determine the dependence of β on length.

Synthesis: The synthetic methodology implemented for the preparation of the NLO chromophores investigated in the present work is based upon the preparation of polyenals of increasing length bearing the electron-donating moieties, followed by grafting of the electron-withdrawing terminal groups (Scheme 2). Thus, molecules of series 1–3a and 1–3b were obtained from Knoevenagel condensation[34] of molecules of series 1–3c [n = 0–3] with either 1,3-diethyl-2-thiobarbituric acid (for derivatives a) or 3-(dicyanomethylidene)-2,3-dihydrobenzothiophene-1,1-dioxide (for derivatives b). Polyenals of series 1–2c [n = 1–3] were prepared from the generic aldehyde 1–2c [n = 0] by stepwise repetition of Wittig oxyprenylation

Figure 3. Limiting resonance forms for molecules 1a[3] and 3b[3]. In both cases, the acceptor stabilizes the charge-separated form.

1) Stepwise preparation of polyenals

2) Knoevenagel condensation
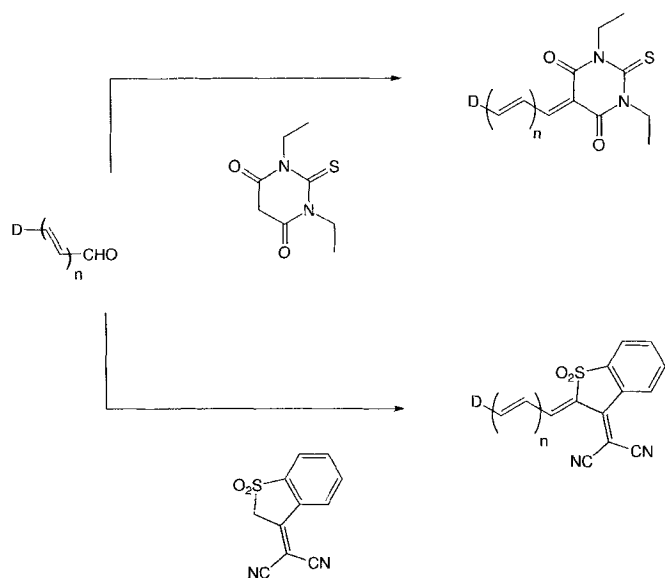
Scheme 2. Synthetic method used for the preparation of polyenes of series 1–3, a–b.

Table 1. Thermal data from DSC experiments for compounds of series 1–3,a–b.

	T_m	T_{di}	T_{dm}
1a[1]	134.8, 189.6	223	234.5
1a[2]	179.5	234	244
1a[3]	177.7	213.5	226
1a[4]	173.8	176	197
1a[5]	172	174	199
1b[1]	177.6	222	236.5
1b[2]	216.6	218.5	228
1b[3]		209	210.5
1b[4]		196.5	199
2a[1]	212.4	216	225.5
2a[2]		214	215
2a[3]		209	210
2a[4]		190	193.5
2a[5]		187	189
2b[1]		233	238
2b[2]		236	242
2b[3]			
2b[4]		196	204
3a[1]	256.3	264	274
3a[2]	238.8	240	241
3a[3]	200.5	201	204
3b[1]		276	278
3b[2]		268	269
3b[3]		232	233.5
3b[4]		208	209.5

followed by acidic hydrolysis.[35] Aldehydes 3c[0] and 3c[1] were obtained by deprotonation of 2-N-piperidinylthiophene with n-butyllithium followed by reaction with DMF (for 3c[0]) or dimethylaminoacrolein (for 3c[1]). Polyenals 3c[2] and 3c[3] were then prepared by bisvinylogous extension of aldehydes 3c[0] and 3c[1] based upon treatment with 1-methoxy-1,3-butadien-4-yl lithium and subsequent acidic hydrolysis.[36]

Thermal stability: Stability is a major requirement for practical applications (in particular for incorporation of NLO chromophores in poled-polymer structures). The thermal stability of the synthetic push–pull polyenes was investigated by differential scanning calorimetry (DSC). Protocols similar to those described in ref. [37] were used. They allowed for determination of T_m (melting point) as well as T_{di} (onset of decomposition) and T_{dm} (maximum of the decomposition exotherm). It should be noted that T_{di} values only provide a helpful upper limit of thermal stability.[37] The DSC data are collected in Table 1.

In a number of cases (in particular for series 2b and 3b as well as higher derivatives of series 1b, 2a, and 3a), decomposition occurs prior to melting. As noted from Table 1, both T_{di} and T_{dm} are found to decrease with increasing polyenic chain length, indicating a decrease of thermal stability for longer polyenic

derivatives. However, thermal decomposition does not occur below 175 °C, even for the longest derivatives. Molecules of type 3 were found to display higher thermal stability than derivatives of type 1 or 2 (in particular for shorter molecules).

Electrochemical properties: In order to evaluate and compare the relative acceptor and donor strength, redox potentials of molecules of similar size incorporating the various donor and acceptor moieties were determined by cyclic voltammetry (CV). All molecules show reversible one-electron oxidation (in some cases two successive one-electron oxidation waves) and reduction waves. The corresponding E^0 values determined relative to the saturated calomel electrode are gathered in Table 2.

Table 2. Redox potential (E^0 values in V relative to SCE) determined by CV.

	Oxidation	Reduction
1a[2]	0.875, 1.830	−0.800
2a[2]	0.730, 1.490	−0.810
3a[2]	0.715	−0.825
1b[2]	0.950, 1.780	−0.384
2b[2]	0.750	−0.440
3b[2]	0.781	−0.490

Comparison of the values for molecules 1a[2], 2a[2], and 3a[2] reveals that the change from dibutylaminophenyl to julolidine and piperidine–thiophene derivatives leads to a decrease of the oxidation potential as well as to a shift of the reduction potential towards more negative values. This is consistent with increasing donor strength that facilitates oxidation and renders reduction more difficult. Conversely, derivatives of type b show both higher oxidation potentials and less negative reduction potentials than molecules of type a, in agreement with the more pronounced acceptor strength (which facilitates reduction and

renders oxidation more difficult) of the 3-(dicyanomethylidene)-2,3-dihydrobenzothiophene-1,1-dioxide moiety compared with the 1,3-diethyl-2-thiobarbituric acid end group.

Ground-state polarization and structure

Polarization: The dipole moment μ of compounds of series 1–3a and 1b were determined from dielectric and refractive index measurements conducted in toluene by means of the Debye formula.[38] Dipole moments of molecules of series 2–3b and 3a could not be satisfactorily investigated by this method owing to their low solubility in apolar solvents. Accordingly, they were determined by electrooptical absorption measurements (vide infra). As can be seen in Table 7, the powerful heterocyclic acceptors induce significant polarization in the ground state.

Comparison of derivatives of series 1a with derivatives of series 1b of similar length indicates that the 3-(dicyanomethylidene)-2,3-dihydrobenzothiophene-1,1-dioxide acceptor moiety leads to slightly smaller dipole moments than the electron-withdrawing 1,3-diethyl-2-thiobarbituric acid end group. However, it should be noted that this effect could be due to the nonlinear shape of the former, in which cyano substituents point back towards the donor. Examination of compounds of series 1a, 2a, 3a reveals that the presence of the piperidine–thiophene donor results in larger dipoles than the julolidine moiety, and that this latter induces larger dipole moments than the dibutyl-aminophenyl group, as expected from the relative donor strengths.

In each homologous series, increasing the conjugation length results in only slight increases in dipole moment, with apparent saturation for the longest derivatives. Such behavior has already been observed with other series of push–pull polyenes.[25, 26] Within the two-form description of push–pull molecules, this behavior can be related to an increase of the contribution of the neutral form to the ground state with increasing length. This reflects the growing difficulty of separating charges over larger distances. As a result, although the dipole moment of the zwitterionic form rises rapidly with length, only a weak increase (or saturation) of the ground-state dipole moment is observed, because of the drop in the zwitterionic contribution to the ground state.

Structure: The molecular structure of molecule 1b[3] in the solid state has been determined by X-ray crystallography. An important feature is that the polyenic chain exhibits a nearly planar zigzag conformation, the heterocyclic and phenyl rings of the acceptor moiety lying in the same average plane. The phenyl ring of the donor moiety is only slightly twisted (twist angle $\approx 16°$) with respect to the plane of the conjugated chain. Similarly, the dicyanovinyl of the acceptor moiety lies almost in the same plane (twist angle $\approx 9°$). Bond length alternation can be directly determined in the solid state by calculating the average difference between $C=C$ and $C-C$ bond lengths in the polyenic chain linking the donor and acceptor moiety. A BLA value of -0.04 Å is obtained, indicative of *reduced bond length alternation* and a significant contribution of the zwitterionic resonance form in the ground state of molecule 1b[3] in the solid state. This is also indicated by the partial quinoidal character of the phenyl ring of the donor end group. X-ray crystallography indicates an almost optimal BLA for

molecule 1b[3] in the solid state. However, it should be kept in mind that in general the solid state corresponds to a polar environment because of the strong internal field in crystals of polar molecules. This will tend to favor charge separation and therefore may be responsible for an alteration of BLA with respect to apolar or weakly polar media.

In order to obtain information about the structure and conformation of molecules 1–3,a–b in an apolar environment, we conducted AM1 semiempirical calculations for the isolated state. These calculations yielded nearly planar conjugated polyenic chains for all polyenic derivatives. The aromatic rings of the three donor moieties (1, 2, or 3) were found to be only slightly twisted with respect to the conjugated chain (except for molecules corresponding to $n = 1$ owing to steric hindrance). For $n > 1$, the thiobarbituric acceptor moiety (molecules of type a) was found to be almost planar and close to the plane of the conjugated chain. In contrast, the calculations suggested an overall "butterfly" shape for molecules of type b. The heterocyclic acceptor moiety is tilted with respect to the polyenic chain. In particular, the dicyanovinyl group presents a twist angle of about 34°. The differences noted between the conformations of the heterocyclic acceptor for molecules of type b in the solid and in the isolated state may be attributed to packing effects that play an important role in determining the conformations of molecules in the crystal.

The AM1 calculations indicate that bond length alternation is more pronounced near the donor end than near the acceptor end. This behavior was also observed in the crystal structure of two push–pull phenylpolyenes bearing a strong heterocyclic acceptor,[19] and probably reflects the larger influence of powerful heterocyclic acceptor end groups than aromatic donor moieties. For that reason, we chose to define BLA as an *average* coordinate. In agreement with a conventional earlier definition, BLA values were calculated as the average difference between adjacent $C=C$ and $C-C$ bond lengths in the polyenic chain. The BLA values obtained for molecules 1–3,a–b in the isolated state are listed in Table 3. They range from -0.055 to -0.09 Å, depending on the donor–acceptor strength as well as on the

Table 3. BLA (average difference between $C=C$ and $C-C$ bonds) from AM1 calculations for compounds of series 1–3,a–b (in Å).

n	1a	2a	3a	1b	2b	3b
1	−0.081	−0.080	−0.057	−0.080	−0.076	−0.055
2	−0.0825	−0.082	−0.073	−0.085	−0.085	−0.078
3	−0.088	−0.087	−0.081	−0.090	−0.089	−0.083
4	−0.090	−.0090	−0.085	−0.092	−0.092	−0.087

polyenic chain length. This is indicative of somewhat reduced bond length alternation. In addition, the bond lengths obtained for the aromatic donor terminal groups are consistent with some contribution of the zwitterionic form in the ground state of the molecules. In particular, the phenyl rings of molecules of type 1 and 2 are found to show partial quinoidal character. An important point is the difference between the BLA values calculated for the isolated molecule 1b[3] and determined in the crystal. A much less alternated structure was obtained in the solid state than in the isolated state; this indicates a notable stabilization of

the zwitterionic form by polar surroundings. Further investigations of the influence of a polar environment on bond length alternation are presented below.

In each series of homologous push–pull polyenes, |BLA| values increase with increasing polyenic chain length. In the two-form description, this behavior can be explained in terms of increasing weight of the neutral form with increasing polyenic chain length, resulting from the larger energetic price associated with charge separation. The behavior is consistent with the leveling-off of the ground-state dipole moment observed with rising polyenic chain length. For compounds of comparable length and bearing identical acceptors, |BLA| is found to decrease in the order series **1** > series **2** > **3**. Thus, increasing donor strength leads to decreasing BLA, in agreement with an increased contribution of the zwitterionic form and concomitant increased ground-state polarization. On the other hand, derivatives of type **b** are found to show slightly more pronounced BLA (except for molecules corresponding to $n = 1$, probably due to steric hindrance preventing planarity in the case of molecules **1a**[1], **2a**[2], and **3a**[2]) than derivatives of type **a**, though the 3-(dicyanomethylidene)-2,3-dihydrobenzothiophene-1,1-dioxide (**b**) was found to be a more powerful electron-withdrawing group than the 1,3-diethyl-2-thiobarbituric moiety (**a**). This peculiar behavior could possibly be explained by the solvent effect on the ground-state structure and the difference in polarizability between the different derivatives (vide infra). In particular, it should be kept in mind that the CV measurements used for ranking of relative acceptor strengths were conducted in a polar solvent, acetonitrile.

NMR studies: ^{1}H NMR spectra obtained in CDCl$_3$ indicated an all-*trans* configuration of the polyenic chain for molecules **1**–**3,a**–**c**. Each proton along the polyenic chain was identified by means of COSY experiments. Their chemical shifts show oscillatory behavior: the odd-row protons (starting from the donor terminal) are deshielded with respect to shielded even-row protons (except for the last even-row proton, which is deshielded because of its proximity to carbonyl or cyano groups responsible for magnetic anisotropy).

Quantum chemical calculations and related NMR investigations conducted on a number of cyanines, merocyanines, and polyenes have revealed an almost linear correlation between the coupling constant for *trans* vicinal protons in the conjugated chain and the corresponding carbon–carbon bond length (or bond order).[39, 40] Accordingly, examination of the variation of the $^3J_{HH}$ values along the polyenic chain provides an estimation of BLA in solution. For an alternated polyene (BLA ≈ − 0.1 Å), the difference (ΔJ) between CH=CH and CH–CH coupling constants amounts to about 6.5 Hz,[39] whereas it vanishes for cyanines (BLA = 0 Å), so that optimum BLA (in terms of quadratic hyperpolarizability) is expected to correspond to ΔJ values amounting to approximately 3 Hz. The $^3J_{HH}$ values determined in CDCl$_3$ for push–pull polyenes of series **1**–**3,a**–**b** are collected in Table 4. ΔJ is found to vary along the polyenic chains, suggesting that bond length alternation tends to decrease from the donor to the acceptor end, in agreement with AM1 calculations. Therefore, we calculated the average ΔJ values ($\overline{\Delta J}$). As clearly seen in Table 4, all $\overline{\Delta J}$ values were significantly smaller than 6 Hz, indicative of reduced bond length

Table 4. ^{1}H–^{1}H coupling constants ($^3J_{HH}$) between vicinal protons measured in CDCl$_3$ along the polyenic chain, and corresponding $\overline{\Delta J}$ values (average difference in $^3J_{HH}$ values across adjacent C=C and C–C bonds) for compounds of series 1–3,a–b.

	$^3J_{HH}$ from the donor end to the acceptor end (in Hz)	$\overline{\Delta J}$ (in Hz)
1a[2]	14.5, 12.5	2.0
1a[3]	14.8, 11.0, 13.4, 12.7	2.2
1a[4]	15.0, 10.4, 14.1, 12.0, 13.4, 12.8	2.4
1a[5]	nd, nd, nd, 11.6, 14.3, 11.9, 13.5, 12.7 [a]	
1b[2]	14.1, 12.2	1.9
1b[3]	14.7, 10.3, 13.4, 11.7	3.0
1b[4]	14.8, 11.1, 14.0, 10.7, 13.7, 11.2	3.2
2a[2]	14.3, 12.7	1.6
2a[3]	15.1, 10.8, 13.3, 12.7	2.5
2a[4]	nd, nd, 14.2, 11.7, 13.7, 12.7	
2a[5]	nd, nd, nd, 11.6, 14.3, 11.7, 13.6, 12.7	
2b[2]	13.5, 12.5	1.0
2b[3]	14.2, 10.3, 13.2, 12.5	2.3
2b[4]	14.65, 10.7, 14.2, 11.2, 13.0, 12.2	2.6
3a[2]	13.4, 12.9	0.5
3a[3]	14.2, 11.9, 13.2, 13.0	1.2
3a[4]	14.3, 11.5, 13.9, 12.0, 13.5, 13.0	1.7
3b[2]	13.0, 13.0	0
3b[3]	12.7, 12.4, 13.0, 12.9	0.2
3b[4]	ins [b]	

[a] nd: not determined due to overlap of proton signals. [b] ins: insoluble.

alternation for push–pull polyenes of series **1**–**3,a**–**b** in chloroform solution. The values ranged from 3 to 0 Hz, depending on the donor–acceptor strength as well as on the polyenic chain length. In contrast, push–pull polyenals of **1**–**3c** showed much more pronounced bond length alternation, an experimental observation consistent with the much smaller acceptor strength of the aldehyde end group. These results emphasize the validity of the approach based upon the use of powerful heterocyclic acceptors that bring some stabilization upon charge separation. In each series of homologous push–pull polyenes $\overline{\Delta J}$ values increase with increasing polyenic chain length, in agreement with more pronounced bond length alternation. Also, $\overline{\Delta J}$ values appear to decrease from series **1** to series **2** then **3**, in agreement with increasing donor strength leading to decreasing bond length alternation (as predicted by AM1 calculations). In particular, the piperidinothiophene donor moiety always yields weakly alternated systems (due to the weaker loss in aromaticity associated with charge separation) when combined with powerful heterocyclic acceptors (series **3a** and **3b**). For instance, molecules **3a**[2], **3b**[2], and **3b**[3] appear to be close to the cyanine limit in CDCl$_3$.

Effect of solvent polarity: Solvent-dependent NMR studies conducted on push–pull polyenes **1**–**3,a**–**b**[2] suggest that the ground-state structure can be significantly affected by solvent polarity (Table 5). When the solvent polarity was increased, the coupling constants between vicinal protons across C=C bonds were found to decrease, whereas the coupling constants across C–C bonds were found concomitantly to increase, indicative of an increased contribution of the zwitterionic form. As a result, ΔJ values decrease significantly with increasing solvent polarity for each compound.

Results of previous experimental NMR studies have shown that the electronic structure of various merocyanine dyes can be modulated by solvent polarity, and are consistent with stabilization of the zwitterionic form by polar solvents.[40 – 43] Such be-

Table 5. Variation of the difference in ^{1}H–^{1}H coupling constants across adjacent C=C and C-C bonds in the polyenic chain in solvents of various polarities: ΔJ values in Hz.

	1a[2]	1b[2]	2a[2]	2b[2]	3a[2]	3b[2]
CCl$_4$	2.4	2.5	2.3	ins [a]	nd [b]	ins
[D$_8$]dioxane	2.3	2.5	2.0	nd	1.0	nd
(CD$_3$)$_2$CO	2.2	nd	1.8	ins	0.9	ins
CDCl$_3$	2.0	1.9	1.6	1.0	0.5	0
(CD$_3$)$_2$SO	1.8	1.2	1.2	0.8	nd	−1.4

[a] ins: insoluble. [b] nd: not determined due to overlap of proton signals.

havior can be explained as follows. Polar compounds orientate and/or polarize surrounding solvent molecules, thus creating an electric reaction field.[44, 45] For polar molecules in polar solvents, significant reaction fields can be attained[45] that, in turn, can polarize the solute molecules. The magnitude of this effect is related to the polarizability of the molecule. Since the linear polarizability peaks for BLA = 0 Å and drops for highly alternated structures,[27, 28] pronounced solvent effects on the structure and polarization of push–pull compounds are expected for polar molecules with reduced bond length alternation. This could be the reason why the structure of the push–pull polyenes investigated in the present work exhibits a distinct sensitivity to solvent polarity.

It should be noted that molecule 1a[2] has smaller ΔJ values than molecule 1b[2] in apolar or weakly polar solvents (CCl$_4$ and dioxane), in agreement with the slightly less alternated structure predicted by AM 1 calculations for isolated molecules of type a as compared to isolated molecules of type b. However, molecule 1a[2] leads to a larger ΔJ value than molecule 1b[2] in polar solvents (such as DMSO). Actually, derivatives of type b have smaller ΔJ values (even negative in the case of 3b[2] in DMSO) than derivatives of type a in polar solvents, indicating a more pronounced contribution of the zwitterionic form in the case of molecules of type b. This is consistent with the more pronounced acceptor strength of b than a revealed by CV measurements performed in acetonitrile ($\varepsilon_r = 36.1$), thus leading to an increased contribution of the zwitterionic form and consequently to smaller ΔJ values.

Optical properties

Absorption: The absorption spectra of the push–pull polyenes investigated in the present work display intense bands in the visible or near-IR region. The wavelengths of the absorption maxima (λ_{max}) measured in various solvents are collected in Table 6. All compounds appear to display *positive* solvatochromism (in particular molecules of series 1–2). Such a solvatochromic behavior is characteristic of ICT transitions with an increase of the dipole moment upon excitation, and can be interpreted in terms of predominance of the neutral form in the ground-state structure.[46] The solvatochromic behavior of compounds of series 3b cannot easily be investigated, since major solubility problems are encountered in apolar or weakly polar solvents, whereas broad bands with poorly defined maxima are obtained in polar solvents. In this case, a possible inversion of solvatochromism (positive solvatochromism followed by negative solvatochromism) cannot be excluded, indicative of the predominance of the neutral form in apolar solvents and of the zwitterionic form in polar solvents. Such behavior is implied by

Table 6. Absorption solvatochromism of compounds of series 1–3,a–b: λ_{max}, nm [a].

	CH	DO	Et$_2$O	AcOEt	THF	AC	AN	DMF	DMSO
1a[1]	479	486	486	494	497	500	502	507	513
1a[2]	546	556	556	569	572	578	581	591	598
1a[3]	561	581	580	598	604	618	621	651	665
1a[4]	596	601	601	613	622	623	624	650	669
1a[5]	597	607	616	616	624	622	622	649	662
1b[1]	575	581	581	587	592	594	595	603	609
1b[2]	647	657	660	671	679	689	688	704	709
1b[3]	ins [b]	721	711	729	741	768	768	792	805
1b[4]	ins	712	719	729	742	760	759	861	886
2a[1]	493	507	503	513	514	522	523	527	533
2a[2]	565	583	582	595	599	613	613	621	629
2a[3]	581	614	623	647	657	681	680	704	716
2a[4]	613	625	629	643	653	670	653	697	720
2a[5]	618	629	638	628	650	655	648	682	694
2b[1]	ins	611	612	619	623	627	626	635	628
2b[2]	ins	693	700	711	720	726	725	734	737
2b[3]	ins	753	768	789	801	816	812	822	825
2b[4]	ins	752	775	795	846	903	898	910	912
3a[1]	498	508	504	507	508	508	509	512	514
3a[2]	582	603	598	610	614	614	614	620	622
3a[3]	596	625	634	688	698	710	713	712	724
3a[4]	606	633	634	659	671	690	814	825	832
3b[1]	ins	611	ins	617	622	620	617	624	626
3b[2]	ins	711	ins	724	728	722	719	728	728
3b[3]	ins	789	ins	826	836	826	818	826	826
3b[4]	ins	769	ins	925	944	923	920		940

[a] CH: cyclohexane; DO: dioxane; AC: acetone; AN: acetonitrile. [b] ins: insoluble.

the solvent-dependent NMR experimental data of molecule 3b[2] (Table 5).

In each series of homologous compounds, a bathochromic shift as well as a broadening of the main absorption band is observed with increasing polyenic chain length, as illustrated in Figure 4. The amplitude of this effect depends on the donor–acceptor groups, as well as on the solvent polarity (see Table 6). Large vinylene shifts are obtained, in particular in polar solvents. This parallels the behavior observed with merocyanine dyes.[47–49] A linear dependence of λ_{max} on the number n of conjugated double bonds in the polyenic chain is observed for series 3a and 1–3b in DMSO, with a regular vinylene shift of about 100 nm.[49] Therefore, *in polar media*, these molecules exhibit comparable absorption behavior to cyanine dyes.[50] In contrast, leveling-off of λ_{max} is observed for the longest derivatives in solvents of low polarity. This compares with the classical behavior of polyenes.[51]

Comparison of molecules of similar length from series 1a, 2a, and 3a (as well as from series 1b, 2b, and 3b) indicates a bathochromic shift on moving from the dibutylaminophenyl to the julolidine or the piperidinothiophene donor moieties, following increasing donor strength or decreasing aromaticity. Likewise, derivatives of type b always show a marked bathochromic shift with respect to derivatives of type a.

Electrooptical absorption measurements: In order to gain further insight into the nature of the ICT transition, we conducted electrooptical absorption measurements (EOAM). EOAMs consist in studying the effect of an external electric field E_0 on the absorption of linearly polarized light by a dilute solution of chromophore.[52] The EOA spectrum is given by Equation (2),

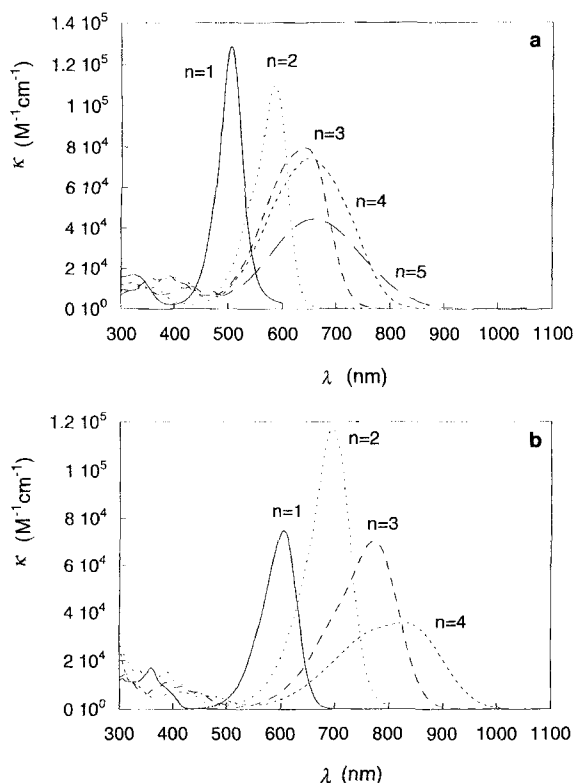$$L\kappa/\tilde{v} = \frac{(\kappa^E/\tilde{v}) - (\kappa/\tilde{v})}{E_0^2} \tag{2}$$

Figure 4. a) Absorption spectra of molecules of series **1a** in chloroform. b) Absorption spectra of molecules of series **1b** in chloroform.

where $\tilde{v}$ is the wavenumber of the optical field and κ^E the extinction coefficient of the solute in the presence of the applied field E_0.

An example of the optical $(\kappa/\tilde{v})$ and electrooptical $(L\kappa/\tilde{v})$ spectra obtained for compound **1a[1]** is shown in Figure 5. The excellent agreement between the experimental and approximated EOA spectra indicates that there is only one intense electronic transition contributing in the region of the lowest-energy transition. A regression analysis of the EOA spectrum gives informa-
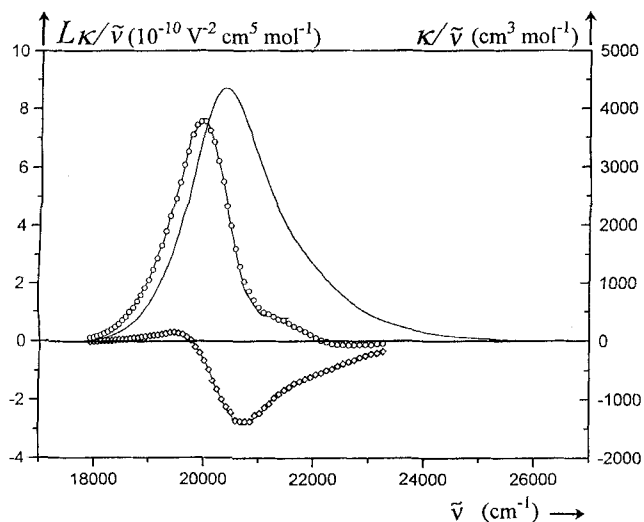

Figure 5. Optical $\kappa/\tilde{v}$ and electrooptical $L\kappa/\tilde{v}$ absorption spectra of molecule **1a[1]** in dioxane at 298 K. The figure shows experimental data points for parallel (o) and perpendicular (◇) polarization of the incident light relative to the external applied electric field and calculated curves obtained by a general least-squares optimization.

tion on the ground- and excited-state dipoles and polarizabilities of the solute.[52] For push–pull molecules with significant ground-state dipole moments and large photoinduced changes of dipole moment, polarizability contributions and terms originating from the field dependence of the transition dipole are usually small. Hence, both the ground-state dipole moment and the photoinduced change of dipole moment (i.e., μ and $\Delta\mu$ values) can be derived.[53, 54] Details of the evaluation are given in ref. [54]. Lorentz-type local field corrections were applied as in ref. [53]. The results obtained in dioxane are presented in Table 7.

Table 7. Dipole moments, absorption, EOAM, and EFISH data for compounds of series **1–3,a–b**.

	μ [a] D	μ_{01} [b] D	$\Delta\mu$ [c] D	$\mu\beta(2\omega)$ [d] 10^{-48} esu	λ_{max} ($\kappa_{max} \times 10^{-4}$) [e] nm (cm^{-1}M^{-1})	$\mu\beta(0)$ [f] 10^{-48} esu	$\beta_\mu(0)$ [g] 10^{-30} esu
1a[1]	7.2	9.3 [h]	7.7 [h]	680	505 (12.8)	455	65
1a[2]	7.9	10.7 [h]	13.2 [h]	2150	587 (11.0)	1210	150
1a[3]	8.6	11.3 [h]	22.1 [h]	5300	641 (8.0)	2580	300
1a[4]	8.8	12.3 [h]	28.7 [h]	9300	650 (7.5)	4400	500
1a[5]	9.0 [h]	13.7 [h]	42.4 [h]	19500 [h]	659 (4.4) [h]	8970 [h]	1000
1b[1]	6.1	8.9	11.9	950	603 (7.5)	510	85
1b[2]	6.9	11	18	5200	695 (11.8)	2110	310
1b[3]	8.2			13500 [i]	773 (7.0)	3870	470
1b[4]	8.3			60000	826 (3.6)	12200	1470
2a[1]	8.25			610 [j]	524 (10.4)	390	50
2a[2]	8.9			2210 [j]	614 (10.9)	1160	130
2a[3]				7150 [j]	681 (9.1)	3060	
2a[4]				19100 [j]	686 (6.6)	8010	
2a[5]				26600	685 (4.3)	11200	
2b[1]	7.0 [k]	7.7	10.2	970	635 (6.6)	480	
2b[2]				5500	734 (17.3)	1910	
2b[3]				22000	821 (14.3)	4635	
2b[4]				abs	895 (8.2)		
3a[1]	9.6 [k]	8.2	1.8	125	512 (16.0)	80	9
3a[2]	10.4 [k]	10.5	6.1	1100	619 (19.1)	570	55
3a[3]				4820	710 (10.4)	1850	
3b[1]	8.9 [k]	8.6	4.1	450 [i]	617 (29.7)	235	26
3b[2]	10.4 [k]	11.2	7.7	2050 [i]	725 (50.5)	740	71
3b[3]				10000 [i]	834 (19.8)	1900	

[a] μ values measured in toluene (0.2998 D $= 10^{-30}$ Cm). [b] μ_{01} values determined from absorption measurement in dioxane. [c] $\Delta\mu$ values derived from EOAM in dioxane. [d] $\mu\beta(2\omega)$ values determined by EFISH at 1.907 μm in chloroform. [e] Absorption maxima (λ_{max}) and corresponding molar extinction coefficients (κ_{max}) measured in chloroform. [f] Static $\mu\beta(0)$ values were derived from $\mu\beta(2\omega)$ values by the two-level approximation (ref. [10]). [g] β_μ is the projection of the quadratic hyperpolarizability tensor on the dipole moment (2.6944×10^{-30} esu $= 10^{-50}$ Cm^{3}V^{-2}). [h] From ref. [25]. [i] From ref. [31]. [j] From ref. [19]. [k] μ values derived from EOAM in dioxane.

As can be seen in Table 7, $\Delta\mu$ values apparently decrease from series **1** to series **2** then **3**, in agreement with a shift towards the cyanine limit (where $\Delta\mu$ vanishes). In particular, molecules **3a[1]** and **3b[1]** show very small $\Delta\mu$ values and are most probably very close to the cyanine limit in dioxane. It should also be emphasized that lengthening the polyenic chain linking the donor to the acceptor end groups results in an *increase* of both μ_{01} and $\Delta\mu$ values, as well as a *decrease* of the transition energy as noted previously,[24, 25] so that significant enhancement of the quadratic hyperpolarizability is expected, based on the two-level approximation [see Eq. (1)].

Optical nonlinearities

Experimental methodology: The molecular optical quadratic nonlinearities of molecules of series **1–3,a–b** were investigated by performing quadratic Electric-Field-Induced-Second-Har-

monic (EFISH) generation experiments in solution.[55–57] The EFISH experiment allows the determination of the mean microscopic hyperpolarizability γ_0 from Equation (3). The first term

$$\gamma_0 = \gamma(-2\omega;\omega,\omega,0) + \mu\beta(-2\omega;\omega,\omega)/5kT \qquad (3)$$

is the scalar part of the cubic hyperpolarizability tensor, while the second originates from the partial orientation of the ground-state dipole μ in the static electric field. Usually, for push–pull polyenes of similar size, the orientational contribution is assumed to be the predominant component. It should be borne in mind that this approximation may not be strictly valid for very long derivatives, since cubic hyperpolarizability is known to increase steeply with length.[15] Yet γ is predicted to cancel for BLA $= -0.05$ Å (when β peaks positively) and peaks *negatively* for BLA $= 0$ Å.[26–28] Since for all the molecules investigated in the present work, γ_0 was found to be large and positive, we have neglected the electronic contribution to γ_0. The scalar product $\mu\beta(2\omega)$—where $\beta(2\omega)$ (a shorthand notation for $\beta(-2\omega;\omega,\omega)$) is the vector part of the quadratic hyperpolarizability tensor— was thus directly inferred.

The results are gathered in Table 7. The experiments were carried out at 1.907 μm in chloroform. Compounds **2b**[4] and **3b**[4] could not be investigated owing to significant absorption at 2ω (i.e., 953 nm). Table 7 gives the $\mu\beta(2\omega)$ values and the static $\mu\beta(0)$ values calculated from the two-level model, since $\beta(2\omega)$ values are significantly affected by dispersion enhancement. The two-level quantum model has proven appropriate to describe push–pull stilbenes[10] and is used here as an approximation to calculate the dispersion enhancement factor [Eq. (4)],

$$\beta = \beta(0)\frac{4\lambda_{max}^2}{(\lambda^2 - \lambda_{max}^2)(\lambda^2 - 4\lambda_{max}^2)} \qquad (4)$$

where λ is the wavelength of the optical field (here 1.907 μm) and λ_{max} the wavelength of the ICT transition.

β_μ values (where β_μ is the projection of the quadratic hyperpolarizability tensor on the dipole moment) have been calculated by dividing the experimental $\mu\beta$ values (derived from EFISH experiments performed in chloroform) by the μ values obtained from dipole moment measurements carried out in toluene. As a result, the β_μ values should be slightly overestimated, since the ground-state polarization depends on the external medium and is expected to increase with solvent polarity as discussed above. Another important point to note is that μ and β are not necessarily parallel, an effect that will tend to reduce β_μ with respect to β. In particular, significant angles are expected for derivatives of type **b**.[58]

Correlation between structure and hyperpolarizability: As discussed previously, calculations predict that for push–pull polyenes β peaks positively for a fixed BLA value (BLA $= -0.05\pm0.01$ Å, which should correspond approximately to $\Delta J \approx 3\pm0.3$ Hz) but drops for highly alternated (i.e., BLA $= \pm0.11$ Å) and cancels for nonalternated structures (BLA $= 0$ Å). Thus, BLA is expected to influence the quadratic hyperpolarizability strongly. Another factor that should play an important role in determining the magnitude of the quadratic hyperpolarizability is the peak amplitude β_{max}. Examination of the calculations carried out on different push–pull systems suggests

that β_{max} markedly depends on the donor–acceptor structure.[26]

Effect of end groups: Let us first compare results obtained for molecules with the same chain length n. Examination of derivatives **1a**[2], **2a**[2], and **3a**[2] (as well as **1b**[2], **2b**[2], and **3b**[2]) bearing the same acceptor but different donors indicates a decrease of the $\mu\beta(0)$ and $\beta_\mu(0)$ values with increasing donor strength and decreasing bond length alternation (see Tables 4 and 7). According to ΔJ values determined in CDCl$_3$, this behavior is consistent with structures showing relatively small bond length alternation in chloroform solution (i.e., -0.05 Å $\le$ BLA ≤ 0 Å) and shifting to the right of the positive β peak with increasing donor strength (Figure 1). For this particular size, the weakest donor, dibutylaminophenyl, leads to the largest quadratic nonlinearities. On the other hand, when considering the longer analogues **1b**[3], **2b**[3], and **3b**[3] (or **1a**[3], **2a**[3], and **3a**[3]), it appears that the $\mu\beta(0)$ values *first* increase *then* decrease with increasing donor strength. For molecules corresponding to $n = 3$, the intermediate julolidine donor leads to the largest nonlinearities (see comparison of molecules **1a**[3], **2a**[3] and **3a**[3] or **1b**[3], **2b**[3] and **3b**[3]). The piperidinothiophene donor appears to be too strong when associated with the powerful heterocyclic acceptors, so that it always induces a smaller BLA. The position of β so far to the right of the positive β peak explains why compound **3a**[n] (or **3b**[n]) yields a smaller $\mu\beta(0)$ value than analogous compounds **1a**[n] and **2a**[n] (or **1b**[n] and **2b**[n]).

As will be noted from Table 7, derivatives of type **b** always show superior nonlinearity to the corresponding molecules of type **a**. In addition, close examination reveals that molecules with acceptor **b** have larger β_{max} values. For instance, molecules **1a**[2] and **1b**[2] display similar ΔJ values in chloroform. Yet compound **1b**[2] yields a $\beta_\mu(0)$ value twice as large as that of compound **1a**[2]. Also, molecule **2a**[2] seems closer to the optimum BLA (according to ΔJ values) than compound **2b**[2]. Nevertheless, the larger $\mu\beta(0)$ value is obtained for the less optimized structure. Such behavior indicates that β peaks at a greater value for the derivative of type **b** than for the derivative of type **a**. This phenomenon is also observed when considering molecules in which $n = 3$. Compounds **2a**[3] and **2b**[3] display similar $\overline{\Delta J}$ values in chloroform, whereas the $\mu\beta(0)$ product is larger for the type **b** derivative. Likewise, compounds **3a**[3] and **3b**[3] display equal nonlinearity. Yet **3b**[3] is closer to the cyanine limit. Finally, molecule **1b**[4] shows an unprecedented nonlinearity, almost 3 times that of **1a**[4], indicative of a huge β_{max} value. Thus, all the results indicate that derivatives of type **b** display much higher β_{max} values than molecules of type **a**.

Length effect: As the entries in Table 7 demonstrate, for each series of homologous compounds lengthening the polyenic chain results in steep increases in both $\mu\beta$, $\mu\beta(0)$, and $\beta_\mu(0)$ values. This leads to particularly large $\mu\beta$ and $\mu\beta(0)$ values for the longest molecules, which suit such molecules for use as guests in poled-polymer films. For instance, the $\mu\beta$ value for molecule **1b**[4] is 100 times that of DANS,[59] a common benchmark for quadratic effects. Molecule **1b**[3] has been shown to lead to a poled polymer with a very large electrooptic coefficient.[31]
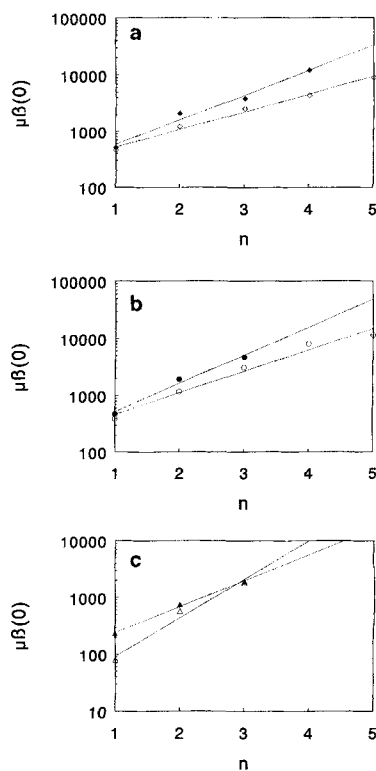
Figure 6. a) Plot of the $\mu\beta(0)$ values versus the number n of double bonds in the polyenic chain for series 1a ($\circ$) and 1b ($\bullet$); all $\mu\beta(0)$ values are expressed in 10^{-48} esu; b) as for Figure 6a for series 2a ($\circ$) and 2b ($\bullet$); c) as for Figure 6a for series 3a ($\triangle$) and 3b ($\blacktriangle$).

The enhancement of $\mu\beta(0)$ as a function of the number n of double bonds in the polyenic chain is shown in Figure 6a for series 1a–b, Figure 6b for series 2a–b, and Figure 6c for series 3a–b. The semilogarithmic plots indicate *exponential* dependencies of $\mu\beta(0)$ on n.[60] Exponential dependencies of $\beta_\mu(0)$ on n are also obtained for series 1a–b. The steep length dependencies can be analyzed in terms of combined effects of variation of β_{max} and BLA as a function of polyenic chain length. Recent semiempirical calculations carried out on a series of push–pull polyenes of increasing length show that all compounds display β versus BLA plots of similar shape but different magnitude. In particular, the *peak magnitude* ($|\beta_{max}|$) increases dramatically with conjugation length.[29] However, experimentally, the dependence of β on length will also be governed by the dependence of the BLA value of molecules with a constant donor and acceptor on the length. An important factor is the BLA value for the shortest D–A molecule in a series. For instance, for push–pull polyenes in which the neutral resonance form predominates in the ground state (i.e., with negative BLA), such as those investigated in the present work, |BLA| tends to increase with increasing polyenic chain length (BLA becomes more negative) owing to the increased contribution of the neutral form in the ground state. If the BLA of the generic compound is in the range $-0.05 < \text{BLA} < 0$ Å, then an increase in the length can move it either closer to the optimal BLA value (i.e., -0.05 Å) or past it, depending on how BLA is affected by increasing chain length. In the first case, a steep increase of $\beta(0)$ will be observed because of both the increase in β_{max} and the shift of BLA values closer to optimal BLA. Experimentally, $\beta(0)$ will then rise faster than β_{max}. In contrast, in the second case (when the generic compound falls in the range $-0.11 < \text{BLA} < -0.05$ Å), $\beta(0)$ will rise more slowly than β_{max}. The steep length plots observed for vinylogous molecules of series 1–3,a–b are most likely of the first type since, according to ΔJ values, the shortest generic compounds have BLA values in the region $-0.05 \ll \text{BLA} \leq 0$ Å, while BLA shifts towards optimum BLA value with increasing polyenic chain length ($1 \leq n \leq 4$).

Conclusion

The design of push–pull polyenes combining aromatic donor groups with powerful heterocyclic acceptors that induce stabilization upon charge separation has proven an effective strategy for approaching the optimum BLA required for maximum quadratic hyperpolarizability. In addition, it has been shown experimentally for the first time that the maximum β value depends heavily on the structure of the end groups. In particular, the 3-(dicyanomethylidenyl)-2,3-dihydrobenzothiophene-2-ylidenyl-1,1-dioxide acceptor was found to induce sharply enhanced quadratic nonlinearities. Hence, molecule 1b[4] shows a huge $\beta_\mu(0)$ value of 1500×10^{-30} esu.

In each series of homologous molecules of increasing length, increasing polyenic chain length enhances quadratic optical nonlinearities exponentially. Thus polyenic chromophores in which the dibutylaminophenyl donor and the 3-(dicyanomethylidenyl)-2,3-dihydrobenzothiophene-2-ylidenyl-1,1-dioxide acceptor are combined display excellent optical quadratic nonlinearities (with $\mu\beta$ values as large as 100 times that of DANS) as well as satisfactory solubility. These combined properties are of particular interest for incorporation as NLO active guests in poled-polymer systems.[31] Further efforts towards an improved efficiency–stability trade-off are in progress.

Experimental procedure

General: All the chemicals and the solvents used in the synthesis were of the highest commercially available quality. Purification by column chromatography was performed on Merck 60 silica gel (0.040–0.063 mm). NMR spectra were recorded with Bruker AM 200 SY, AM 400 SY, or AM 500 SY apparatus. Elemental analyses were performed by the Service Régional de Microanalyses, Paris (France). Mass spectra were recorded at the Ecole Normale Supérieure, Paris (France) under chemical ionization conditions. Fast atom bombardment (FAB) mass spectra were recorded by the mass spectrometry facility of University of California at Riverside. Melting points were measured by differential scanning calorimetry with a Perkin–Elmer DSC7 microcalorimeter. The DSC records were obtained at $20\,^\circ\text{C}\,\text{min}^{-1}$ in air in a sealed pan.

Cyclic voltammetry was performed by means of a classical three-electrode cell working under argon, with 10^{-3}M solutions of chromophores in distilled acetonitrile in tetrabutylammonium tetrafluoroborate 0.3 M as the supporting electrolyte. The cyclic voltammograms were recorded at $500\,\text{mVs}^{-1}$ with a platinum working electrode (diameter 0.5 mm) and a saturated calomel electrode (SCE) as the reference electrode. E^0 values were determined with platinum ultramicroelectrodes (diameter 10 μm) in a stationary regime at $20\,\text{mVs}^{-1}$. The number of electrons involved in each redox process was measured with ferrocene as an internal reference.[61]

The ground-state dipole moments were determined by means of a cylindrical dipole meter and a 1689 M Digibridge GENRAD capacitance bridge. The measurements were carried out in dry toluene. The experimental error amounts to less than 5%.

The electronic absorption spectra were recorded with a Beckman DU 600, DU 7400, or a Perkin–Elmer 340 spectrophotometer. The solvatochromic behavior was investigated in analytical grade solvents. The molar decadic extinction coefficients κ were obtained according to the Lambert–Beer equation. The transition dipoles μ_{01} were determined by numerical integration of the absorption bands as defined in refs. [62,63], with the inclusion of a Lorentz local field correction. EOAM measurements were performed at $T = 298$ K in dioxane carefully purified and dried by column chromatography on basic alumina followed by distillation over sodium/potassium alloy under argon. The experimental error range is 1–5%. The electrooptical absorption device is described in ref. [64].

EFISH measurements were conducted with a Q-switched Nd^{3+}:YAG laser that emitted pulses of about 8 ns duration at 1.064 µm. This emission was shifted to 1.907 µm by a hydrogen Raman cell at 40 bar. These experiments were performed with solutions of increasing concentration in chloroform for each molecule. The measurements were calibrated relative to a quartz wedge. For the quartz reference, the experimental value of the quadratic susceptibility $d_{11} = 1.2 \times 10^{-19}$ esu determined at 1.06 µm was used. To account for dispersion, this value is extrapolated to $d_{11} = 1.1 \times 10^{-19}$ esu at 1.91 µm. The cubic contribution to the EFISH signal was neglected. The experimental accuracy range is 5–10%.

General procedure for the synthesis of derivatives 1–3a: 1,3-diethyl-2-thiobarbituric acid (200 mg, 1 mmol) was dissolved in refluxing absolute ethanol (50 mL). An aldehyde of series 1–3c (1 mmol) was added and the solution was then allowed to cool to room temperature and stirred for 6 h while protected from light and moisture. A dark suspension was obtained. The crude condensation product was collected by filtration followed by rinsing with ethanol, ether, and pentane. If necessary, the product was purified by column chromatography (eluting with methylene chloride), then crystallized in a CH_2Cl_2/EtOH mixture.

Compound 1a[1]: Yield 89%; ^1H NMR (200 MHz, $CDCl_3$, 25°C, TMS): $\delta = 8.41$ (d, $^3J(H,H) = 7.6$ Hz, 2H), 8.40 (s, 1H), 6.67 (d, $^3J(H,H) = 9.4$ Hz, 2H), 4.60 (2q, $^3J(H,H) = 7.0$ Hz, 4H), 3.41 (t, $^3J(H,H) = 7.5$ Hz, 4H), 1.52–1.71 (m, 4H), 1.28–1.47 (m, 10H), 0.98 (t, $^3J(H,H) = 7.1$ Hz, 6H); MS (CI, NH_3): m/z: 416 [$M+H^+$]; $C_{23}H_{33}N_3O_2S$ (415.6): calcd C 66.47, H 8.00, N 10.11; found C 66.65, H 8.11, N 10.19.

Compound 1a[2]: Yield 96%; ^1H NMR (200 MHz, $CDCl_3$, 25°C, TMS): $\delta = 8.45$ (dd, $^3J(H,H) = 14.3$, 12.6 Hz, 1H), 8.20 (d, $^3J(H,H) = 12.5$ Hz, 1H), 7.60 (d, $^3J(H,H) = 9.0$ Hz, 2H), 7.44 (d, $^3J(H,H) = 14.6$ Hz, 1H), 6.63 (d, $^3J(H,H) = 9.0$ Hz, 2H), 4.56, 4.57 (2q, $^3J(H,H) = 6.9$ Hz, 4H), 3.38 (t, $^3J(H,H) = 7.5$ Hz, 4H), 1.55–1.66 (m, 4H), 1.26–1.44 (m, 10H), 0.98 (t, $^3J(H,H) = 7.1$ Hz, 6H); MS (CI, NH_3): m/z: 442 [$M+H^+$]; $C_{25}H_{35}N_3O_2S$ (441.6): calcd C 67.99, H 7.99, N 9.51; found C 67.97, H 8.07, N 9.41.

Compound 1a[3]: Yield 68%; ^1H NMR (400 MHz, $CDCl_3$, 25°C, TMS): $\delta = 8.13$ (d, $^3J(H,H) = 12.7$ Hz, 1H), 8.03 (t, $^3J(H,H) = 13.0$ Hz, 1H), 7.40 (d, $^3J(H,H) = 8.8$ Hz, 2H), 7.35 (dd, $^3J(H,H) = 13.4$, 11.0 Hz, 1H), 7.06 (d, $^3J(H,H) = 14.65$ Hz, 1H), 6.95 (dd, $J = 14.9$, 11.0 Hz, 1H), 6.62 (d, $^3J(H,H) = 9.3$ Hz, 2H), 4.57, 4.55 (2q, $^3J(H,H) = 6.9$ Hz, 4H), 3.34 (t, $^3J(H,H) = 7.8$ Hz, 4H), 1.60 (m, 4H), 1.27–1.42 (m, 10H), 0.97 (t, $^3J(H,H) = 7.3$ Hz, 6H); MS (CI, NH_3): m/z: 468 [$M+H^+$]; $C_{27}H_{37}N_3O_2S$ (467.7): calcd C 69.34, H 7.98, N 8.98; found C 69.14, H 7.99, N 9.06.

Compound 1a[4]: Yield 82%; ^1H NMR (400 MHz, $CDCl_3$, 25°C, TMS): $\delta = 8.09$ (d, $^3J(H,H) = 12.8$ Hz, 1H), 7.99 (t, $^3J(H,H) = 13.4$ Hz, 1H), 7.35 (d, $^3J(H,H) = 8.6$ Hz, 2H), 7.25 (dd, $^3J(H,H) = 13.4$, 11.8 Hz, 1H), 6.96 (dd, $^3J = 14.2$, 10.4 Hz, 1H), 6.87 (d, $^3J(H,H) = 15.0$ Hz, 1H), 6.76–6.82 (m, 1H), 6.60 (d, $^3J(H,H) = 9.1$ Hz, 2H), 6.57 (dd, $^3J(H,H) = 13.9$, 12.3 Hz, 1H), 4.54 (q, $^3J(H,H) = 7.0$ Hz, 4H), 3.32 (t, $^3J(H,H) = 7.5$ Hz, 4H), 1.59 (q, $^3J(H,H) = 7.5$ Hz, 4H), 1.36 (sext, $^3J(H,H) = 7.5$ Hz, 4H), 1.27–1.32 (t, $^3J(H,H) = 6.5$ Hz, 4H), 0.96 (t, $^3J(H,H) = 7.5$ Hz, 6H); MS (CI, NH_3): m/z: 494 [$M+H^+$]; $C_{29}H_{39}N_3O_2S$ (493.7): calcd C 70.55, H 7.96, N 8.51; found C 70.45, H 8.29, N 8.61.

Compound 1a[5]: Yield 43%; ^1H NMR (400 MHz, $CDCl_3$, 25°C, TMS): $\delta = 8.08$ (d, $^3J(H,H) = 12.7$ Hz, 1H), 7.99 (t, $^3J(H,H) = 13.5$, 12.8 Hz, 1H), 7.31 (d, $^3J(H,H) = 8.9$ Hz, 2H), 7.22 (dd, $^3J(H,H) = 13.5$, 12.0 Hz, 1H), 6.88 (dd, $^3J = 14.25$, 11.6 Hz, 1H), 6.77 (m, 1H), 6.72 (m, 2H), 6.59 (d, $^3J(H,H) = 8.8$ Hz, 2H), 6.55 (dd, $^3J(H,H) = 14.3$, 11.9 Hz, 1H), 6.44 (t, $^3J(H,H) = 12.6$, 12.38 Hz, 1H), 4.54 (q, $^3J(H,H) = 6.9$ Hz, 4H), 3.30 (t, $^3J(H,H) = 7.5$ Hz, 4H), 1.58 (m, 4H), 1.27 (m, 10H), 0.96 (t, $^3J(H,H) = 7.2$ Hz, 6H); $C_{31}H_{41}N_3O_2S$ (519.75): calcd C 71.64, H 7.95, N 8.08; found C 71.62, H 7.93, N 8.02.

Compound 2a[1]: Yield 97%; ^1H NMR (200 MHz, $CDCl_3$, 25°C, TMS): $\delta = 8.28$ (s, 1H), 8.06 (brs, 2H), 4.61, 4.58 (2q, $^3J(H,H) = 7.0$ Hz, 4H), 3.40 (t, $^3J(H,H) = 5.8$ Hz, 4H), 2.79 (t, $^3J(H,H) = 6.0$ Hz, 4H), 1.99 (quint, $^3J(H,H) = 6.0$ Hz, 4H), 1.33, 1.31 (2t, $^3J(H,H) = 7.0$ Hz, 6H); MS (CI, NH_3): m/z: 386 [$M+H^+$]; $C_{21}H_{25}N_3O_2S$ (383.5): calcd C 65.77, H 6.57, N 10.96; found C 65.88, H 6.53, N 10.89.

Compound 2a[2]: Yield 98%; ^1H NMR (200 MHz, $CDCl_3$, 25°C, TMS): $\delta = 8.40$ (dd, $^3J(H,H) = 14.1$, 12.9 Hz, 1H), 8.17 (d, $^3J(H,H) = 12.7$ Hz, 1H), 7.37 (d, $^3J(H,H) = 14.3$ Hz, 1H), 7.23 (brs, 2H), 4.51–4.64 (2q, 4H), 3.35 (t, $^3J(H,H) = 5.7$ Hz, 4H), 2.75 (t, $^3J(H,H) = 6.1$ Hz, 4H), 1.97 (quint, $^3J(H,H) = 5.9$ Hz, 4H), 1.33, 1.30 (2t, $^3J(H,H) = 6.9$ Hz, 6H); MS (CI, NH_3): m/z: 410 [$M+H^+$]; $C_{23}H_{27}N_3O_2S$ (409.5): calcd C 67.45, H 6.65, N 10.26; found C 67.50, H 6.68, N 10.18.

Compound 2a[3]: Yield 86%; ^1H NMR (400 MHz, $CDCl_3$, 25°C, TMS): $\delta = 8.11$ (d, $^3J(H,H) = 12.7$ Hz, 1H), 8.01 (app. t, $^3J(H,H) = 13.2$ Hz, 1H), 7.33 (dd, $^3J(H,H) = 13.4$, 11.0 Hz, 1H), 7.01 (brs, 2H), 7.00 (d, $^3J(H,H) = 15.1$ Hz, 1H), 6.92 (dd, $^3J(H,H) = 15.1$, 10.7 Hz, 1H), 4.56, 4.55 (2q, $^3J(H,H) = 7.0$ Hz, 4H), 3.30 (t, $^3J(H,H) = 5.6$ Hz, 4H), 2.74 (t, $^3J(H,H) = 6.3$ Hz, 4H), 1.97 (quint, $^3J(H,H) = 6.0$ Hz, 4H), 1.31, 1.29 (2t, $^3J(H,H) = 6.8$ Hz, 6H); MS (CI, NH_3): m/z: 436 [$M+H^+$]; $C_{25}H_{29}N_3O_2S$ (435.6): calcd C 68.94, H 6.71, N 9.65; found C 68.94, H 6.76, N 9.53.

Compound 2a[4]: Yield 89%; ^1H NMR (400 MHz, $CDCl_3$, 25°C, TMS): $\delta = 8.09$ (d, $^3J(H,H) = 12.7$ Hz, 1H), 7.98 (dd, $^3J(H,H) = 13.7$, 12.7 Hz, 1H), 7.25 (dd, $^3J(H,H) = 13.7$, 11.7 Hz, 1H), 6.97 (brs, 2H), 6.96 (ddd, $^3J(H,H) = 14.5$, 11.5, 3.0 Hz, 1H), 6.76 (m, 2H), 6.55 (dd, $^3J(H,H) = 14.2$, 11.7 Hz, 1H), 4.54, 4.53 (2q, $^3J(H,H) = 7.0$ Hz, 4H), 3.26 (t, $^3J(H,H) = 5.6$ Hz, 4H), 2.74 (t, $^3J(H,H) = 6.3$ Hz, 4H), 1.96 (quint, $^3J(H,H) = 6.0$ Hz, 4H), 1.31, 1.29 (2t, $^3J(H,H) = 6.8$ Hz, 6H); MS (CI, NH_3): m/z: 462 [$M+H^+$]; $C_{27}H_{31}N_3O_2S + 0.1 CH_2Cl_2$: calcd C 69.13, H 6.68, N 8.92; found C 69.14, H 6.71, N 8.99.

Compound 2a[5]: Yield 82%; ^1H NMR (400 MHz, $CDCl_3$, 25°C, TMS): $\delta = 8.07$ (d, $^3J(H,H) = 12.7$ Hz, 1H), 7.99 (dd, $^3J(H,H) = 13.5$, 12.8 Hz, 1H), 7.22 (dd, $^3J(H,H) = 13.6$, 11.8 Hz, 1H), 6.92 (brs, 2H), 6.88 (dd, $^3J(H,H) = 14.3$, 11.6 Hz, 1H), 6.74 (m, 1H), 6.68 (m, 2H), 6.54 (dd, $^3J(H,H) = 14.3$, 11.7 Hz, 1H), 6.42 (dd, $^3J(H,H) = 13.3$, 11.7 Hz, 1H), 4.55 (q, $^3J(H,H) = 7.0$ Hz, 4H), 3.24 (t, $^3J(H,H) = 5.6$ Hz, 4H), 2.76 (t, $^3J(H,H) = 6.3$ Hz, 4H), 1.99 (quint, 4H), 1.33 (t, 6H); $C_{29}H_{33}N_3O_2S + 0.085 CH_2Cl_2$: calcd C 70.51, H 6.75, N 8.48; found C 70.51, H 6.78, N 8.21.

Compound 3a[1]: Yield 95%; ^1H NMR (200 MHz, $CDCl_3$, 25°C, TMS): $\delta = 8.29$ (s, 1H), 7.65 (d, $^3J(H,H) = 5.1$ Hz, 1H), 6.41 (d, $^3J(H,H) = 5.1$ Hz, 1H), 4.59 (q, $^3J(H,H) = 7.0$ Hz, 4H), 3.64 (br t, 4H), 1.77 (m, 6H), 1.33, 1.31 (2t, $^3J(H,H) = 6.9$ Hz, 6H); MS (CI, NH_3): m/z: 378 [$M+H^+$]; $C_{18}H_{23}N_3O_2S_2$ (377.5): calcd C 57.27, H 6.14, N 11.13; found C 57.40, H 6.36, N 11.07.

Compound 3a[2]: Yield 66%; ^1H NMR (500 MHz, $CDCl_3$, 25°C, TMS): $\delta = 8.05$ (d, $^3J(H,H) = 12.9$ Hz, 1H), 7.96 (app. t, $^3J(H,H) = 13.1$ Hz, 1H), 7.48 (d, $^3J(H,H) = 13.4$ Hz, 1H), 7.35 (br d, $^3J(H,H) = 4.6$ Hz, 1H), 6.20 (d, $^3J(H,H) = 4.7$ Hz, 1H), 4.58, 4.56 (2q, $^3J(H,H) = 6.85$ Hz, 4H), 3.49 (t, $^3J(H,H) = 5.0$ Hz, 4H), 1.74 (m, 6H), 1.32, 1.29 (2t, $^3J(H,H) = 6.9$ Hz, 6H); MS (CI, NH_3): m/z: 404 [$M+H^+$]; $C_{20}H_{25}N_3O_2S_2$ (403.6): calcd C 59.53, H 6.24, N 10.41; found C 59.44, H 6.49, N 10.21.

Compound 3a[3]: Yield 68%; ^1H NMR (500 MHz, $CDCl_3$, 25°C, TMS): $\delta = 8.05$ (d, $^3J(H,H) = 13.0$ Hz, 1H), 7.96 (t, $^3J(H,H) = 13.2$ Hz, 1H), 7.27 (dd, $^3J(H,H) = 13.2$, 12.0 Hz, 1H), 7.17 (d, $^3J(H,H) = 14.2$ Hz, 1H), 7.11 (d, $^3J(H,H) = 4.4$ Hz, 1H), 6.50 (dd, $^3J(H,H) = 14.1$, 11.8 Hz, 1H), 6.07 (d, $^3J(H,H) = 4.4$ Hz, 1H), 4.56 (2q, $^3J(H,H) = 6.9$ Hz, 4H), 3.39 (t, $^3J(H,H) = 5.5$ Hz, 4H), 1.74 (quint, $^3J(H,H) = 5.3$ Hz, 4H), 1.69 (m, 2H), 1.31, 1.29 (2t, $^3J(H,H) = 7.0$ Hz, 6H); MS (CI, NH_3): m/z: 430 [$M+H^+$]; $C_{22}H_{27}N_3O_2S_2$ (429.6): calcd C 61.51, H 6.33, N 9.78; found C 61.51, H 6.40, N 9.68.

Compound 3a[4]: Yield 66%; ^1H NMR (500 MHz, $CDCl_3$, 25°C, TMS): $\delta = 8.06$ (d, $^3J(H,H) = 13.0$ Hz, 1H), 7.96 (t, $^3J(H,H) = 13.0$ Hz, 1H), 7.22 (dd, $^3J(H,H) = 13.5$, 12.0 Hz, 1H), 6.94 (br d, 1H), 6.93 (d, $^3J(H,H) = 14.2$ Hz, 1H), 6.90 (dd, $^3J(H,H) = 13.9$, 11.5 Hz, 1H), 6.50 (dd, $^3J(H,H) = 13.85$, 12.05 Hz, 1H), 6.36 (dd, $^3J(H,H) = 14.5$, 11.5 Hz, 1H), 5.98 (d, $^3J(H,H) = 4.2$ Hz, 1H), 4.54 (q, $^3J(H,H) = 6.8$ Hz, 4H), 3.30 (t, $^3J(H,H) = 5.5$ Hz, 4H), 1.72 (m, 4H), 1.64 (m, 2H), 1.30, 1.29 (2t, $^3J(H,H) = 7.0$ Hz, 6H); $C_{24}H_{29}N_3O_2S_2$ (455.6): calcd C 63.27, H 6.42, N 9.22; found C 63.20, H 6.63, N 8.90.

General procedure for the synthesis of derivatives 1–3b: 3-(dicyano-methylidenyl)-2,3-dihydrobenzothiophene-2-ylidenyl-1,1-dioxide (115 mg, 0.5 mmol) was dissolved in refluxing absolute ethanol (100 mL). An aldehyde of series **1–3c** (0.5 mmol) was added, and the solution was then allowed to cool to room temperature and stirred for 6 h protected from light and moisture. A dark suspension was obtained. The crude condensation product was collected by filtration, followed by rinsing with ethanol, ether, and pentane. The product was either obtained pure or purified by column chromatography (eluting with methylene chloride), then crystallized in a CH_2Cl_2/EtOH mixture.

Compound 1b[1]: Yield 69%; ^1H NMR (200 MHz, $CDCl_3$, 25°C, TMS): $\delta = 8.80$ (m, 1H), 8.33 (s, 1H), 7.90–8.00 (m, 3H), 7.75–7.85 (m, 2H), 6.74 (d, ^3J(H,H) = 9.0 Hz, 2H), 3.45 (t, ^3J(H,H) = 7.5 Hz, 4H), 1.60–1.75 (m, 4H), 1.30–1.50 (m, 4H), 1.00 (t, ^3J(H,H) = 7.1 Hz, 6H); MS (CI, NH_3): m/z: 446 $[M+H^+]$; $C_{26}H_{27}N_3O_2S$ (445.6): calcd C 70.10, H 6.10, N 9.40; found C 69.91, H 6.22, N 9.40.

Compound 1b[2]: Yield 75%; ^1H NMR (200 MHz, $CDCl_3$, 25°C, TMS): $\delta = 8.80$–8.90 (m, 1H), 8.61 (d, ^3J(H,H) = 12.2 Hz, 1H), 7.90–8.00 (m, 1H), 7.70–7.83 (m, 2H), 7.60 (dd, ^3J(H,H) = 14.0, 12.3 Hz, 1H), 7.59 (d, ^3J(H,H) = 8.8 Hz, 2H), 7.35 (d, ^3J(H,H) = 14.1 Hz, 1H), 6.87 (d, ^3J(H,H) = 8.9 Hz, 2H), 3.41 (t, ^3J(H,H) = 7.4 Hz, 4H), 1.54–1.73 (m, 4H), 1.30–1.50 (m, 4H), 0.99 (t, ^3J(H,H) = 7.2 Hz, 6H); MS (CI, NH_3): m/z: 472 $[M+H^+]$; $C_{28}H_{29}N_3O_2S$ (471.6): calcd C 71.31, H 6.20, N 8.91; found C 70.98, H 6.13, N 8.90.

Compound 1b[3]: Yield 82%; ^1H NMR (400 MHz, $CDCl_3$, 25°C, TMS): $\delta = 8.84$ (d, ^3J(H,H) = 7.3 Hz, 1H), 8.52 (d, ^3J(H,H) = 11.7 Hz, 1H), 7.93–7.95 (m, 1H), 7.75–7.81 (m, 2H), 7.44 (d, ^3J(H,H) = 8.8 Hz, 2H), 7.33 (dd, ^3J(H,H) = 13.7, 11.0 Hz, 1H), 7.28 (dd, ^3J(H,H) = 13.2, 10.3 Hz, 1H), 7.12 (d, ^3J(H,H) = 14.7 Hz, 1H), 7.01 (dd, ^3J(H,H) = 14.7, 10.3 Hz, 1H), 6.63 (d, ^3J(H,H) = 8.8 Hz, 2H), 3.37 (t, ^3J(H,H) = 7.3 Hz, 4H), 1.62 (quint, ^3J(H,H) = 7.5 Hz, 4H), 1.38 (sext, ^3J(H,H) = 7.3 Hz, 4H), 0.98 (t, ^3J(H,H) = 7.3 Hz, 6H); MS (CI, NH_3): m/z: 498 $[M+H^+]$; $C_{30}H_{31}N_3O_2S$ +0.08CH_2Cl_2: calcd C 71.54, H 6.22, N 8.32; found C 71.54, H 6.16, N 8.39.

Compound 1b[4]: Yield 97%; ^1H NMR (400 MHz, $CDCl_3$, 25°C, TMS): $\delta = 8.83$ (d, ^3J(H,H) = 7.3 Hz, 1H), 8.48 (d, ^3J(H,H) = 11.2 Hz, 1H), 7.94 (d, ^3J(H,H) = 7.6 Hz, 1H), 7.75–7.82 (m, 2H), 7.38 (d, ^3J(H,H) = 8.8 Hz, 2H), 7.22–7.30 (m, 2H), 7.02 (dd, ^3J(H,H) = 13.9, 11.0 Hz, 1H), 6.92 (d, ^3J(H,H) = 15.1 Hz, 1H), 6.83 (dd, ^3J(H,H) = 14.6, 11.2 Hz, 1H), 6.64 (dd, ^3J(H,H) = 14.2, 10.7 Hz, 1H), 6.60 (d, ^3J(H,H) = 8.8 Hz, 2H), 3.33 (t, ^3J(H,H) = 7.6 Hz, 4H), 1.53–1.64 (m, ^3J(H,H) = 7.3 Hz, 4H), 1.39 (sext, ^3J(H,H) = 7.3 Hz, 4H), 0.97 (t, ^3J(H,H) = 7.3 Hz, 6H); MS (CI, NH_3): m/z: 524 $[M+H^+]$; $C_{32}H_{33}N_3O_2S$ (523.7): calcd C 73.39, H 6.35, N 8.02; found: C 73.26, H 6.19, N 8.01.

Compound 2b[1]: Yield 88%; ^1H NMR (200 MHz, $CDCl_3$, 25°C, TMS): $\delta = 8.79$ (m, 1H), 8.21 (s, 1H), 7.92 (m, 1H), 7.61 (br s, 2H), 7.70–7.85 (m, 2H), 3.45 (t, ^3J(H,H) = 5.9 Hz, 4H), 2.81 (t, ^3J(H,H) = 6.1 Hz, 4H), 2.00 (quint, ^3J(H,H) = 5.6 Hz, 4H); MS (CI, NH_3): m/z: 414 $[M+H^+]$; $C_{24}H_{19}N_3O_2S$ +0.2CH_2Cl_2: calcd C 67.00, H 4.52, N 9.67; found C 67.04, H 4.58, N 9.58.

Compound 2b[2]: Yield 97%; ^1H NMR (200 MHz, $CDCl_3$, 25°C, TMS): $\delta = 8.83$–8.87 (m, 1H), 8.59 (d, ^3J(H,H) = 12.5 Hz, 1H), 7.90–7.95 (m, 1H), 7.73–7.78 (m, 2H), 7.54 (dd, ^3J(H,H) = 13.5, 12.5 Hz, 1H), 7.27 (d, ^3J(H,H) = 13.5 Hz, 1H), 7.21 (br s, 2H), 3.42 (t, ^3J(H,H) = 5.7 Hz, 4H), 2.77 (t, ^3J(H,H) = 6.2 Hz, 4H), 2.00 (quint, ^3J(H,H) = 5.2 Hz, 4H); MS (CI, NH_3): m/z: 440 $[M+H^+]$; $C_{26}H_{21}N_3O_2S$ +0.06CH_2Cl_2: calcd C 70.37, H 4.79, N 9.44; found C 70.37, H 4.79, N 9.35.

Compound 2b[3]: Yield 73%; ^1H NMR (400 MHz, $CDCl_3$, 25°C, TMS): $\delta = 8.84$ (d, ^3J(H,H) = 8.8 Hz, 1H), 8.51 (d, ^3J(H,H) = 12.2 Hz, 1H), 7.90–7.94 (m, 1H), 7.73–7.78 (m, 2H), 7.32 (dd, ^3J(H,H) = 13.2, 10.3 Hz, 1H), 7.24 (app. t, ^3J(H,H) = 13 Hz, 1H), 7.08 (br s, 2H), 7.06 (d, ^3J(H,H) = 14.2 Hz, 1H), 6.97–7.07 (m, 1H), 3.36 (t, ^3J(H,H) = 5.6 Hz, 4H), 2.75 (t, ^3J(H,H) = 6.3 Hz, 4H), 1.98 (quint, ^3J(H,H) = 6 Hz, 4H); MS (CI, NH_3): m/z: 466 $[M+H^+]$; $C_{28}H_{23}N_3O_2S$ (465.6): calcd C 72.24, H 4.98, N 9.03; found C 72.09, H 4.73, N 9.19.

Compound 2b[4]: Yield 97%; ^1H NMR (400 MHz, $CDCl_3$, 25°C, TMS): $\delta = 8.83$ (m, 1H), 8.47 (m X of ABX, 1H), 7.94 (m, 1H), 7.78 (m, 2H), 7.23 (m AB of ABX, 1H), 7.035 (dd, ^3J(H,H) = 14.2, 10.7 Hz, 1H), 7.005 (br s, 2H), 6.88 (d, ^3J(H,H) = 14.65 Hz, 1H), 6.81 (dd, ^3J(H,H) = 14.65, 10.7 Hz, 1H), 6.62 (app. ddd, ^3J(H,H) = 14.2, 11.2, 3.0 Hz, 1H), 3.30 (t, ^3J(H,H) = 5.9 Hz, 4H), 2.74 (t, ^3J(H,H) = 6.3 Hz, 4H), 1.97 (quint, ^3J(H,H) = 6.0 Hz, 4H); MS (CI, NH_3): m/z: 492 $[M+H^+]$; $C_{30}H_{25}N_3O_2S$ (491.6): calcd C 73.30, H 5.13, N 8.55; found C 73.30, H 4.93, N 8.47.

Compound 3b[1]: Yield 71%; ^1H NMR (200 MHz, $CDCl_3$, 25°C, TMS): $\delta = 8.83$ (m, 1H), 8.66 (br s, 1H), 7.88 (m, 1H), 7.70–7.76 (m, 2H), 7.60 (br d, 1H), 6.42 (br d, 1H), 3.67 (br t, 4H), 1.81 (m, 6H); MS (CI, NH_3): m/z: 408 $[M+H^+]$; $C_{21}H_{17}N_3O_2S_2$ (407.5): calcd C 61.90, H 4.20, N 10.31; found C 61.68, H 4.24, N 10.24.

Compound 3b[2]: Yield 83%; ^1H NMR (200 MHz, $CDCl_3$, 25°C, TMS): $\delta = 8.84$ (m, 1H), 8.48 (d, ^3J(H,H) = 13.0 Hz, 1H), 7.88 (m, 1H), 7.66–7.75 (m, 2H), 7.46, 7.45 (br d + d, ^3J(H,H) = 13.0 Hz, 2H), 6.99 (br t, ^3J(H,H) = 13.0 Hz, 1H), 6.35 (d, ^3J(H,H) = 4.9 Hz, 1H), 3.61 (t, ^3J(H,H) = 5.4 Hz, 4H), 1.80 (m, 6H); MS (CI, NH_3): m/z: 434 $[M+H^+]$; $C_{23}H_{19}N_3O_2S_2$ (433.5): calcd C 63.72, H 4.42, N 9.69; found C 63.33, H 4.39, N 9.66.

Compound 3b[3]: Yield 51%; ^1H NMR (500 MHz, $CDCl_3$, 25°C, TMS): $\delta = 8.82$ (m, 1H), 8.42 (d, ^3J(H,H) = 12.9 Hz, 1H), 7.89 (m, 1H), 7.66–7.78 (m, 2H), 7.31 (d, ^3J(H,H) = 4.7 Hz, 1H), 7.25 (d, ^3J(H,H) = 12.7 Hz, 1H), 7.24 (app. t, ^3J(H,H) = 12.4 Hz, 1H), 7.11 (app. t, ^3J(H,H) = 13.0 Hz, 1H), 6.54 (app. t, ^3J(H,H) = 12.7 Hz, 1H), 6.25 (d, ^3J(H,H) = 4.7 Hz, 1H), 3.54 (t, ^3J(H,H) = 5.4 Hz, 4H), 1.77 (m, 6H); MS (CI, NH_3): m/z: 460 $[M+H^+]$; $C_{25}H_{21}N_3O_2S_2$ +0.25CH_2Cl_2: calcd C 63.08, H 4.51, N 8.74; found C 63.18, H 4.56, N 8.75.

Compound 3b[4]: Yield 100%; MS (CI, NH_3): m/z: 486 $[M+H^+]$; $C_{27}H_{23}N_3O_2S_2$ +0.20CH_2Cl_2: calcd C 65.00, H 4.69, N 8.36; found C 64.87, H 4.85, N 8.32.

Preparation of polyenals 1–2c: The generic aldehydes **1c[0]** and **2c[0]** were obtained by formylation of dibutylaniline (for **1c[0]**)[65] or julolidine (**2c[0]**) by the classical Vilsmeier–Haack reaction.[66]

Aldehyde 2c[0]: Yield 80%; ^1H NMR (200 MHz, $CDCl_3$, 25°C, TMS): $\delta = 9.59$ (s, 1H), 7.29 (s, 2H), 3.29 (t, ^3J(H,H) = 5.8 Hz, 4H), 2.77 (t, ^3J(H,H) = 6.3 Hz, 4H), 1.96 (quint, ^3J(H,H) = 5.6 Hz, 4H); $C_{13}H_{15}NO$ (201.3): calcd C 77.58, H 7.51, N 6.96; found C 77.48, H 7.51, N 6.94.

Polyenals of series 1–2c were prepared by stepwise vinylogous extension of the generic aldehydes **1–2c[0]**. Repetition of the Wittig oxyprenylation followed by the acid hydrolysis methodology reported in ref. [35] yielded polyenals of increasing size with satisfactory yields according to the following protocol: aldehyde **1–2c[n]** (1 mmol) and 1,3-dioxan-2-yltributylphosphonium bromide[35] (1.1 equiv, 406 mg, 1.1 mmol) were dissolved in anhydrous THF (15 mL). Sodium hydride (1.5 mmol) was added and the suspension was stirred at room temperature in the presence of a catalytic amount of 18-O-6 crown ether for 20 h. After addition of water, the reaction mixture was extracted with ether. The solvent was evaporated, and the crude product was dissolved in THF (10 mL). Hydrochloric acid (10%, 10 ml) was added and the solution was stirred at room temperature for 1 h. After addition of water, the reaction mixture was extracted with methylene chloride; the solvent was evaporated and the residue dried over sodium sulfate, then the crude product was purified by column chromatography (eluting with methylene chloride) to yield pure aldehyde **1–2c[n+1]**.

Aldehyde 1c[1]: Yield 80%; ^1H NMR (200 MHz, $CDCl_3$, 25°C, TMS): $\delta = 9.57$ (d, ^3J(H,H) = 7.9 Hz, 1H), 7.42 (d, ^3J(H,H) = 8.9 Hz, 2H), 7.36 (d, ^3J(H,H) = 15.4 Hz, 1H), 6.62 (d, ^3J(H,H) = 9.0 Hz, 2H), 6.51 (dd, ^3J(H,H) = 15.6, 8.0 Hz, 1H), 3.32 (t, ^3J(H,H) = 7.6 Hz, 4H), 1.59 (m, 4H), 1.36 (sext, ^3J(H,H) = 7.9 Hz, 4H), 0.97 (t, ^3J(H,H) = 7.5 Hz, 6H); $C_{17}H_{25}NO$ (259.4): calcd C 78.72, H 9.71, N 5.40; found C 78.69, H 9.83, N 5.36.

Polyenal 1c[2]: Yield 72%; ^1H NMR (200 MHz, $CDCl_3$, 25°C, TMS): $\delta = 9.54$ (d, ^3J(H,H) = 8.1 Hz, 1H), 7.36 (d, ^3J(H,H) = 8.8 Hz, 2H), 7.25 (dd, ^3J(H,H) = 14.8, 10.6 Hz, 1H), 6.93 (d, ^3J(H,H) = 15.2 Hz, 1H), 6.79

(dd, ^3J(H,H) = 15.1, 10.4 Hz, 1 H), 6.60 (d, ^3J(H,H) = 8.8 Hz, 2 H), 6.18 (dd, ^3J(H,H) = 14.8, 8.1 Hz, 1 H), 3.31 (t, ^3J(H,H) = 7.5 Hz, 4 H), 1.58 (quint, ^3J(H,H) = 7.4 Hz, 4 H), 1.36 (sext, ^3J(H,H) = 7.5 Hz, 4 H), 0.96 (t, ^3J(H,H) = 7.1 Hz, 6 H); $C_{19}H_{27}NO$ (285.4): calcd C 79.95, H 9.54, N 4.91; found C 79.84, H 9.58, N 4.77.

Polyenal 1c[3]: Yield 72%; ^{1}H NMR (200 MHz, CDCl$_3$, 25 °C, TMS): δ = 9.55 (d, ^3J(H,H) = 8.1 Hz, 1 H), 7.33, 7.32 (m + d, ^3J(H,H) = 8.9 Hz, 3 H), 7.18 (dd, ^3J(H,H) = 15.1, 11.3 Hz, 1 H), 6.78 (m, 1 H), 6.70 (m, 1 H), 6.45 (app. t, ^3J(H,H) = 13.9, 11.5 Hz, 1 H), 6.13 (dd, ^3J(H,H) = 15.0, 8.1 Hz, 1 H), 3.30 (t, ^3J(H,H) = 7.5 Hz, 4 H), 1.57 (m, 4 H), 1.36 (sext, ^3J(H,H) = 6.7 Hz, 4 H), 0.96 (t, ^3J(H,H) = 7.2 Hz, 6 H); $C_{21}H_{29}NO$ (311.5): calcd C 80.99, H 9.38, N, 4.50; found C 80.67, H 9.45, N 4.32.

Polyenal 1c[4]: Yield 99%; ^{1}H NMR (400 MHz, CDCl$_3$, 25 °C, TMS): δ = 9.53 (d, ^3J(H,H) = 8.0 Hz, 1 H), 7.29 (d, ^3J(H,H) = 8.9 Hz, 2 H), 7.16 (dd, ^3J(H,H) = 15.05, 11.35 Hz, 1 H), 6.76 (dd, ^3J(H,H) = 14.6, 11.2 Hz, 1 H), 6.61–6.68 (m, 3 H), 6.59 (d, ^3J(H,H) = 8.9 Hz, 2 H), 6.43 (dd, ^3J(H,H) = 14.6, 11.4 Hz, 1 H), 6.36 (dd, ^3J(H,H) = 14.0, 11.3 Hz, 1 H), 6.14 (dd, ^3J(H,H) = 15.0, 8.0 Hz, 1 H), 3.29 (t, ^3J(H,H) = 7.5 Hz, 4 H), 1.50–1.67 (m, 4 H), 1.35 (sext, 4 H), 0.96 (t, ^3J(H,H) = 7.2 Hz, 6 H); $C_{23}H_{31}NO$ + 0.06 CH$_2$Cl$_2$: calcd C 80.73, H 9.14, N 4.08; found C 80.73, H 9.25, N 4.12.

Polyenal 2c[1]: Yield 99%; ^{1}H NMR (200 MHz, CDCl$_3$, 25 °C, TMS): δ = 9.55 (d, ^3J(H,H) = 7.9 Hz, 1 H), 7.27 (d, ^3J(H,H) = 15.5 Hz, 1 H), 7.01 (br s, 2 H), 6.47 (dd, ^3J(H,H) = 15.5, 7.9 Hz, 2 H), 3.26 (t, ^3J(H,H) = 5.7 Hz, 4 H), 2.74 (t, ^3J(H,H) = 6.3 Hz, 4 H), 1.96 (quint, ^3J(H,H) = 6.3 Hz, 4 H); $C_{15}H_{17}NO$ (227.3): calcd C 79.26, H 7.54, N 6.16; found C 79.10, H 7.47, N 6.08.

Polyenal 2c[2]: Yield 80%; ^{1}H NMR (200 MHz, CDCl$_3$, 25 °C, TMS): δ = 9.52 (d, ^3J(H,H) = 8.2 Hz, 1 H), 7.22 (dd, ^3J(H,H) = 15.0, 9.5 Hz, 1 H), 6.96 (br s, 2 H), 6.70–6.90 (m, 2 H), 6.14 (dd, ^3J(H,H) = 15.5, 8.5 Hz, 1 H), 3.23 (t, ^3J(H,H) = 5.6 Hz, 4 H), 2.74 (t, ^3J(H,H) = 6.3 Hz, 4 H), 1.96 (m, 4 H); $C_{17}H_{19}NO$ (253.3): calcd C 80.60, H 7.56, N 5.53; found C 80.33, H 7.40, N 5.48.

Polyenal 2c[3]: Yield 65%; ^{1}H NMR (200 MHz, CDCl$_3$, 25 °C, TMS): δ = 9.52 (d, ^3J(H,H) = 8.1 Hz, 1 H), 7.17 (dd, ^3J(H,H) = 15.0, 11.3 Hz, 1 H), 6.92 (br s, 2 H), 6.64–6.88 (m, 3 H), 6.42 (dd, ^3J(H,H) = 13.7, 11.3 Hz, 1 H), 6.11 (dd, ^3J(H,H) = 15.0, 8.0 Hz, 1 H), 3.21 (t, ^3J(H,H) = 5.6 Hz, 4 H), 2.74 (t, ^3J(H,H) = 6.3 Hz, 4 H), 1.96 (quint, ^3J(H,H) = 5.8 Hz, 4 H); $C_{19}H_{21}NO$ (279.4): calcd C 81.68, H 7.58, N 5.01; found C 81.62, H 7.66, N 4.91.

Polyenal 2c[4]: Yield 50%; ^{1}H NMR (400 MHz, CDCl$_3$, 25 °C, TMS): δ = 9.53 (d, ^3J(H,H) = 7.95 Hz, 1 H), 7.15 (dd, ^3J(H,H) = 15.0, 11.3 Hz, 1 H), 6.88 (br s, 2 H), 6.74 (dd, ^3J(H,H) = 14.6, 11.2 Hz, 1 H), 6.50–6.68 (m, 3 H), 6.43 (dd, ^3J(H,H) = 14.6, 11.4 Hz, 1 H), 6.32 (dd, ^3J(H,H) = 14.2, 11.3 Hz, 1 H), 6.14 (dd, ^3J(H,H) = 15.0, 8.0 Hz, 1 H), 3.20 (t, ^3J(H,H) = 5.7 Hz, 4 H), 2.76 (t, 4 H), 1.96 (quint, 4 H); $C_{21}H_{23}NO$ (305.417): calcd C 82.59, H 7.59, N 4.59; found C 82.41, H 7.68, N 4.87.

Preparation of aldehydes 3c[0] and 3c[1]: n-Butyllithium (9.4 mL, 24 mmol, 2.5 M in hexanes) was added to a solution of 2-N-piperidinylthiophene (3.0 g, 18 mmol) in anhydrous THF (45 mL) at −78 °C. The reaction mixture was stirred for 1 h at −78 °C. A solution of N,N-dimethylformamide (1.94 mL, 1.83 g, 25 mmol) or of 3-(dimethylamino)acrolein (2.5 mL, 2.48 g, 25 mmol) in THF was then added and the reaction mixture brought to room temperature and stirred for 15 min. Hydrochloric acid (9 mL, 3 M) was added and the reaction mixture stirred for 30 min before the pH of the mixture was raised with 10% sodium hydroxide, and the mixture extracted with methylene chloride. The organic layer was washed twice with brine, dried over magnesium sulfate, and filtered. After evaporation of the solvent, the crude product was purified by column chromatography (eluting with methylene chloride) to yield pure aldehyde 3c[0] or 3c[1].

Aldehyde 3c[0]: Yield 80%; ^{1}H NMR (200 MHz, CDCl$_3$, 25 °C, TMS): δ = 9.51 (s, 1 H), 7.47 (d, ^3J(H,H) = 4.4 Hz, 1 H), 6.05 (d, ^3J(H,H) = 4.5 Hz, 1 H), 3.33 (m, 4 H), 1.68 (m, 6 H); $C_{10}H_{13}NOS$ (195.3): calcd C 61.51, H 6.71, N 7.17; found: C 61.40, H 6.60, N 7.33.

Aldehyde 3c[1]: Yield 82%; ^{1}H NMR (200 MHz, CDCl$_3$, 25 °C, TMS): δ = 9.44 (d, ^3J(H,H) = 8.0 Hz, 1 H), 7.41 (d, ^3J(H,H) = 15.0 Hz, 1 H), 7.09 (d, ^3J(H,H) = 4.3 Hz, 1 H), 6.08 (dd, ^3J(H,H) = 15.0, 8.0 Hz, 1 H), 6.00 (d, ^3J(H,H) = 4.3 Hz, 1 H), 3.29 (t, ^3J(H,H) = 5.1 Hz, 4 H), 1.75 (m, 4 H), 1.7 (m, 2 H); HRMS (FAB) m/z: calcd for $C_{12}H_{15}NOS$: 221.0865; found 221.0874.

Polyenal 3c[2]: Yield 62%; (4-methoxy-1,3-butadienyl)tri-n-butylstannane (2.1 mL, 7.5 mmol) was added to anhydrous THF (15 mL) at −78 °C, followed by n-butyllithium (3 mL, 7.5 mmol, 2.5 M in hexanes). The solution was stirred for 1 h at −78 °C. A saturated solution of 3c[0] (0.56 g, 2.8 mmol) in anhydrous THF was then added, and the reaction mixture stirred for 0.5 h while allowed to reach room temperature. After addition of hydrochloric acid (5 mL, 3 M), the reaction mixture was stirred for 0.5 h, rendered basic with 10% sodium hydroxide, extracted with methylene chloride (3 × 25 mL), and washed with water (1 × 25 mL). The emulsion was broken by filtering through Celite, and the organic layer washed again with water (1 × 25 mL) then dried with magnesium sulfate and filtered. After solvent evaporation, the crude orange solid (3.71 g) was purified by column chromatography, eluting with methylene chloride, leading to 0.44 g of pure aldehyde. ^{1}H NMR (500 MHz, CDCl$_3$, 25 °C, TMS): δ = 9.51 (d, ^3J(H,H) = 8.1 Hz, 1 H), 7.17 (dd, ^3J(H,H) = 14.9, 11.3 Hz, 1 H), 6.99 (d, ^3J(H,H) = 14.8 Hz, 1 H), 6.91 (d, ^3J(H,H) = 4.1 Hz, 1 H), 6.38 (dd, ^3J(H,H) = 14.8, 11.3 Hz, 1 H), 6.09 (dd, ^3J(H,H) = 14.8, 8.1 Hz, 1 H), 5.95 (d, ^3J(H,H) = 4.1 Hz, 1 H), 3.25 (m, 4 H), 1.71 (m, 4 H), 1.62 (m, 2 H); HRMS (FAB) m/z: calcd 247.1037; found 247.1031; $C_{14}H_{17}NOS$ (247.4): calcd C 67.98, H 6.93, N 5.66, S 12.96; found C 67.96, H 7.00, N 5.68, S 12.94.

Polyenal 3c[3]: Yield 50%. (4-methoxy-1,3-butadienyl)tri-n-butylstannane (1.9 mL, 6.8 mmol) was added to anhydrous THF (12 mL) at −78 °C, followed by n-butyllithium (2.7 mL, 6.8 mmol, 2.5 M in hexanes). The solution was stirred for 1 h at −78 °C. A saturated solution of 3c[1] (1.0 g, 4.5 mmol) in anhydrous THF was than added, and the reaction mixture stirred for 0.5 h while allowed to reach room temperature. After addition of hydrochloric acid (5 mL, 3 M), the reaction mixture was stirred for 1 h, rendered basic with sodium hydroxide (10%), and washed with a 3/1 brine/potassium fluoride solution. The organic layer was dried with magnesium sulfate and filtered. Solvent evaporation gave 3 g of red solid, which was purified by column chromatography (methylene chloride eluent) to yield 0.61 g of pure aldehyde 3c[3]. ^{1}H NMR (500 MHz, CDCl$_3$, 25 °C, TMS): δ = 9.51 (d, ^3J(H,H) = 8.1 Hz, 1 H), 7.13 (dd, ^3J(H,H) = 15, 11.4 Hz, 1 H), 6.79 (d, ^3J(H,H) = 4.4 Hz, 1 H), 6.78 (d, ^3J(H,H) = 14.9 Hz, 1 H), 6.72 (dd, ^3J(H,H) = 14.5, 11.1 Hz, 1 H), 6.37 (dd, ^3J(H,H) = 14.4, 11.4 Hz, 1 H), 6.30 (dd, ^3J(H,H) = 15.0, 11.0 Hz, 1 H), 6.08 (dd, ^3J(H,H) = 15.0, 8.0 Hz, 1 H), 5.91 (d, ^3J(H,H) = 4.0 Hz, 1 H), 3.21 (m, 4 H), 1.69 (m, 4 H), 1.58 (m, 2 H); HRMS (FAB) m/z: calcd 273.1196; found 273.1187; $C_{16}H_{19}NOS$ + 0.2 H$_2$O: calcd C 69.38, H 7.06, N 5.06, S 11.57; found C 69.38, H 7.06, N 4.96, S 11.40.

[1] *Nonlinear Optical Properties of Organic Molecules and Crystals, Vols. 1 and 2* (Eds.: D. S. Chemla, J. Zyss), Academic Press, New York, **1987**.

[2] *Nonlinear Optical Properties of Polymers* (Eds.: A. J. Heeger, J. Oreinstein, D. R. Ulrich), MRS Symposium Proceedings *109*, Materials Research Society, Pittsburgh, **1988**.

[3] *Nonlinear Optical and Electroactive Polymers* (Eds.: P. N. Prasad, D. R. Ulrich), Plenum, New York, **1988**.

[4] *Organic Materials for Nonlinear Optics* (Eds.: R. A. Hann, D. Bloor), Royal Society of Chemistry, London, **1989**.

[5] *Nonlinear Optical Effects in Organic Polymers* (Eds.: J. Messier, F. Kajzar, P. N. Prasad, D. R. Ulrich), Kluwer Academic, Dordrecht (The Netherlands), **1989**.

[6] *Materials for Nonlinear Optics: Chemical Perspectives* (Eds.: S. R. Marder, J. E. Sohn, G. D. Stucky), ACS Symp. Ser. *455*, American Chemical Society, Washington, **1991**.

[7] P. N. Prasad, D. J. Williams, *Introduction to Nonlinear Optical Effects in Molecules and Polymers*, Wiley, New York, **1991**.

[8] M. Blanchard-Desce, S. R. Marder, M. Barzoukas, in *Comprehensive Supramolecular Chemistry, Vol. 10* (Ed.: D. N. Reinhoudt), Elsevier, Oxford, **1996**, p. 833.

[9] J.-L. Oudar, D. S. Chemla, *J. Chem. Phys.* **1977**, *66*, 2664.

[10] J.-L. Oudar, *J. Chem. Phys.* **1977**, *67*, 446.

[11] M. Barzoukas, M. Blanchard-Desce, D. Josse, J.-M. Lehn, J. Zyss, *Chem. Phys.* **1989**, *133*, 323.

[12] R. A. Huijts, G. L. J. Hesselink, *Chem. Phys. Lett.* **1989**, *156*, 209.

[13] M. Barzoukas, M. Blanchard-Desce, D. Josse, J.-M. Lehn, J. Zyss, in *Materials for Nonlinear and Electro-Optics* (Ed.: M. H. Lyons), Inst. Phys. Conf. Ser. *103*, IOP, Bristol, **1989**, p. 239.

[14] L. T. Cheng, W. Tam, S. R. Marder, A. E. Stiegman, G. Rikken, C. W. Spangler, *J. Phys. Chem.* **1991**, *95*, 10643.

[15] J. Messier, F. Kajzar, C. Sentein, M. Barzoukas, J. Zyss, M. Blanchard-Desce, J.-M. Lehn, *Nonlinear Optics* **1992**, *2*, 53.

[16] B. G. Tiemann, L.-T. Cheng, S. R. Marder, *J. Chem. Soc. Chem. Commun.* **1993**, 735.

[17] S. R. Marder, C. B. Gorman, B. G. Tiemann, L.-T. Cheng, *J. Am. Chem. Soc.* **1993**, *115*, 3006.

[18] M. Blanchard-Desce, J.-M. Lehn, M. Barzoukas, I. Ledoux, J. Zyss, *Chem. Phys.* **1994**, *181*, 281.

[19] S. R. Marder, L.-T. Cheng, B. G. Tiemann, A. C. Friedli, M. Blanchard-Desce, J. W. Perry, J. Skindhøj, *Science* **1994**, *263*, 511.

[20] S. R. Marder, B. G. Tiemann, A. C. Friedli, E. Yang, L.-T. Cheng, *Nonlinear Optics* **1995**, *9*, 213.

[21] M. Blanchard-Desce, J.-M. Lehn, M. Barzoukas, C. Runser, A. Fort, I. Ledoux, J. Zyss, *Nonlinear Optics* **1995**, *10*, 23.

[22] M. Blanchard-Desce, C. Runser, A. Fort, M. Barzoukas, J.-M. Lehn, V. Bloy, V. Alain, *Chem. Phys.* **1995**, *199*, 253.

[23] T. Brotin, C. Andraud, I. Ledoux, S. Brasselet, J. Zyss, M. Perrin, A. Thozet, A. Collet, *Chem. Mater.* **1996**, *4*, 890.

[24] M. Blanchard-Desce, R. Wortmann, S. Lebus, J.-M. Lehn, P. Krämer, *Chem. Phys. Lett.* **1995**, *243*, 526.

[25] M. Blanchard-Desce, V. Alain, L. Midrier, R. Wortmann, S. Lebus, C. Glania, P. Krämer, A. Fort, J. Muller, M. Barzoukas, *J. Photochem. Photobiol. A*, in press.

[26] C. B. Gorman, S. R. Marder, *Proc. Natl. Acad. Sci. U. S. A.* **1993**, *90*, 11297.

[27] S. R. Marder, C. B. Gorman, F. Meyers, J. W. Perry, G. Bourhill, J.-L. Brédas, B. M. Pierce, *Science* **1994**, *265*, 632.

[28] F. Meyers, S. R. Marder, B. M. Pierce, J.-L. Brédas, *J. Am. Chem. Soc.* **1994**, *116*, 10703.

[29] C. B. Gorman, S. R. Marder, *Chem. Mater.* **1995**, *7*, 215.

[30] M. Barzoukas, C. Runser, A. Fort, M. Blanchard-Desce, *Chem. Phys. Lett.* **1996**, *257*, 531.

[31] M. Ahleim, M. Barzoukas, P. V. Bedworth, M. Blanchard-Desce, A. Fort, Z.-Y. Hu, S. R. Marder, J. W. Perry, C. Runser, M. Staehelin, B. Zysset, *Science* **1996**, *271*, 335.

[32] V. Alain, A. Fort, M. Barzoukas, C.-T. Chen, M. Blanchard-Desce, S. R. Marder, J. W. Perry, *Inorg. Chim. Acta* **1996**, *242*, 43.

[33] V. Alain, M. Blanchard-Desce, C.-T. Chen, S. R. Marder, A. Fort, M. Barzoukas, *Synth. Met.* **1996**, *81*, 133.

[34] *Organic Reactions, Vol. 15* (Ed.: R. Adams), Wiley, New York, **1967**.

[35] C. W. Spangler, R. K. McCoy, *Syn. Commun.* **1988**, *18*, 51.

[36] R. H. Wollenburg, *Tetrahedron Lett.* **1978**, 717.

[37] R. J. Twieg, D. M. Burland, J. Hedrick, V. Y. Lee, R. D. Miller, C. R. Moylan, C. M. Seymour, W. Volksen, C. A. Walsh, *Proc. SPIE* **1994**, *2143*, 2.

[38] P. Debye, *Polar Molecules*, Dover, New York, **1945**.

[39] G. Scheibe, W. Seiffert, G. Hohlneicher, C. Jutz, H. J. Springer, *Tetrahedron Lett.* **1966**, 5053.

[40] S. Radeglia, S. Dähne, *J. Mol. Struct.* **1970**, *5*, 399.

[41] R. Radeglia, G. Engelhardt, E. Lippmaa, T. Pehk, K.-D. Nolte, S. Dähne, *Org. Magn. Reson.* **1972**, *4*, 571.

[42] M. Wähnert, S. Dähne, *J. Prakt. Chem.* **1976**, *318*, 321.

[43] I. Baraldi, S. Ghelli, Z. A. Krasnaya, F. Momicchioli, A. S. Tatikolov, D. Vanossi, G. Ponterini, *J. Photochem. Photobiol. A*, to be published.

[44] L. Onsager, *J. Am. Chem. Soc.* **1936**, *58*, 1486.

[45] C. Böttcher, *Theory of Electric Polarization*, Elsevier, Amsterdam, **1973**, p. 63.

[46] C. Reichardt, *Solvents and Solvent Effects in Organic Chemistry*, 2nd ed., VCH, Weinheim (Germany), **1988**, p. 295.

[47] S. Dähne, R. Radeglia, *Tetrahedron* **1971**, *27*, 3673.

[48] S. Schneider, *Ber. Bunsenges. Phys. Chem.* **1976**, *80*, 218.

[49] J. Fabian, H. Hartmann, *Light Absorption of Organic Colorants*, Springer, Berlin, **1981**, pp. 163, 192, and references cited therein.

[50] W. König, *Z. Angew. Chem.* **1925**, *38*, 743.

[51] B. E. Kohler, *J. Chem. Phys.* **1990**, *93*, 5838.

[52] W. Liptay in *Excited States, Vol. 1* (Ed.: C. Lim), Academic Press, New York, **1974**, p. 129.

[53] F. Würthner, F. Effenberger, R. Wortmann, P. Kramer, *Chem. Phys.* **1993**, *173*, 305.

[54] R. Wortmann, P. Krämer, C. Glania, S. Lebus, N. Detzer, *Chem. Phys.* **1993**, *173*, 99.

[55] B. F. Levine, C. G. Bethea, *J. Chem. Phys.* **1975**, *63*, 2666.

[56] I. Ledoux, J. Zyss, *Chem. Phys.* **1982**, *73*, 203.

[57] M. Barzoukas, D. Josse, P. Fremaux, J. Zyss, J.-F. Nicoud, J. O. Morley, *J. Opt. Soc. Am. B* **1987**, *14*, 977.

[58] Preliminary AM1 calculations in the MOPAC package indicate an angle of about 37° for derivatives of series **1b** and **2b**, whereas derivatives of series **1a** and **2a** give an angle of only 10° (M. Lequan, personal communication).

[59] M. Barzoukas, A. Fort, G. Klein, C. Serbutoviez, L. Oswald, J.-F. Nicoud, *Chem. Phys.* **1992**, *164*, 395.

[60] The experimental data can also be fitted with power law dependencies ($\mu\beta(0)\propto n^a$ and $\beta(0)\propto n^{a'}$) leading to a exponent values of 1.8, 2.2, 2.15, 2.05, 2.85, and 1.9, respectively, for series **1a**, **1b**, **2a**, **2b**, **3a**, and **3b** and a' exponent values of 1.65 and 1.9 for series **1a** and **1b**.

[61] C. Amatore, M. Azzabi, P. Calas, A. Jutand, C. Lefrou, Y. Rollin, *J. Electroanal. Chem.* **1990**, *288*, 45.

[62] W. Liptay, *Angew. Chem. Int. Ed. Engl.* **1969**, *8*, 177.

[63] W. Liptay, *Z. Naturforsch.* **1965**, *20a*, 1441.

[64] W. Baumann, *Ber. Bunsenges. Phys. Chem.* **1976**, *80*, 231.

[65] A. Ulman, C. S. Willand, W. Köhler, D. R. Robello, D. J. Williams, L. Handley, *J. Am. Chem. Soc.* **1990**, *112*, 7083.

[66] A. Vilsmeier, A. Haack, *Ber. Dtsch. Chem. Ges.* **1927**, *60*, 121.